

A PRESENTATION OF DOCTORAL DISSERTATION

Department of Mechanical Engineering, University of Ulsan, Korea

Title:

A Sensorless Reflecting Control for Bilateral Haptic Teleoperation System based on Pneumatic Artificial Muscle Actuators



Ph. D candidate: Cong Phat Vo
Advisor: Professor Kyoung Kwan Ahn

Fluid Power Control and Machine Intelligence Laboratory

1

Introduction

2

Modeling and platform setup based on a APAM configuration

3

Adaptive Gain ITSMC with TDE scheme for the position control

4

Adaptive Finite-Time Force Sensorless Control scheme with TDE

5

Model-free control for Optimal contact force in Unknown Environment

6

Optimized Human-Robot Interaction control using IRL

7

Force Sensorless Reflecting Control for BHTS

8

Conclusion and Future works

1

Introduction

2

Modeling and platform setup based on the APAM configuration

3

Adaptive Gain ITSMC with TDE scheme

4

Adaptive Finite-Time Force Sensorless Control scheme with TDE

5

Model-free control for Optimal contact force in Unknown Environment

6

Optimized Human-Robot Interaction force using IRL

7

Force Sensorless Reflecting Control for BHTS

8

Conclusion and Future works

Overview of the BHTS structure

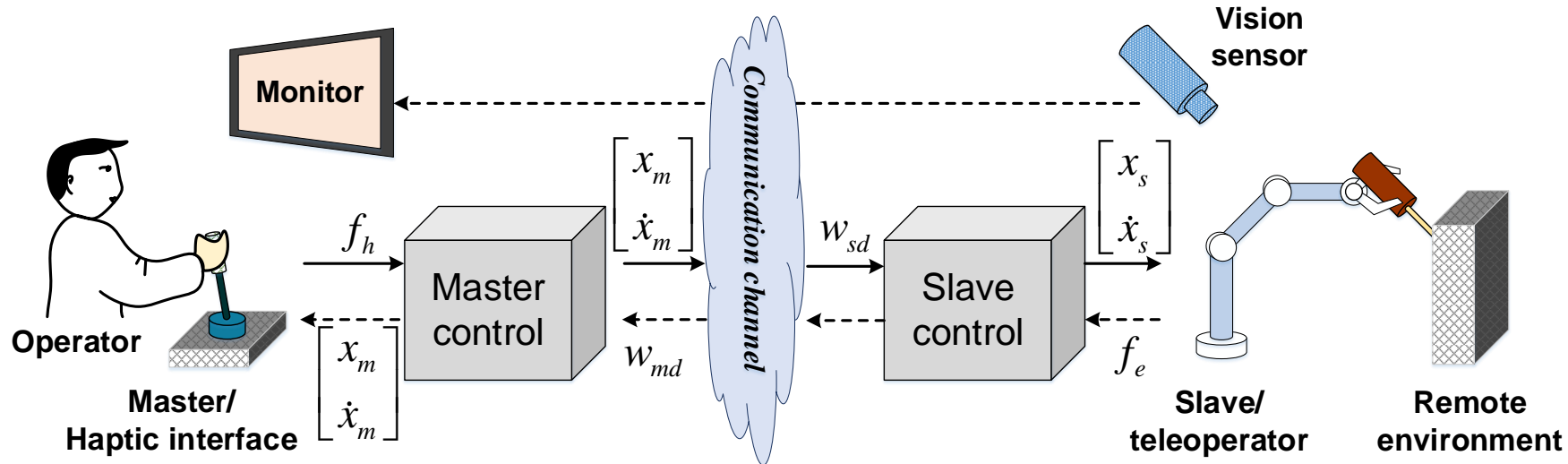


Figure 1.1. The bilateral haptic teleoperation architecture.



Robustness
Performance
Perception
Transparency
 ...

The controllers are **required** to be **robustly stable** with respect to a specified set of uncertainties introduced by the different components. (operator, environment, communication channel, as well as sensors introduce uncertainties)

Overview of the BHTS structure

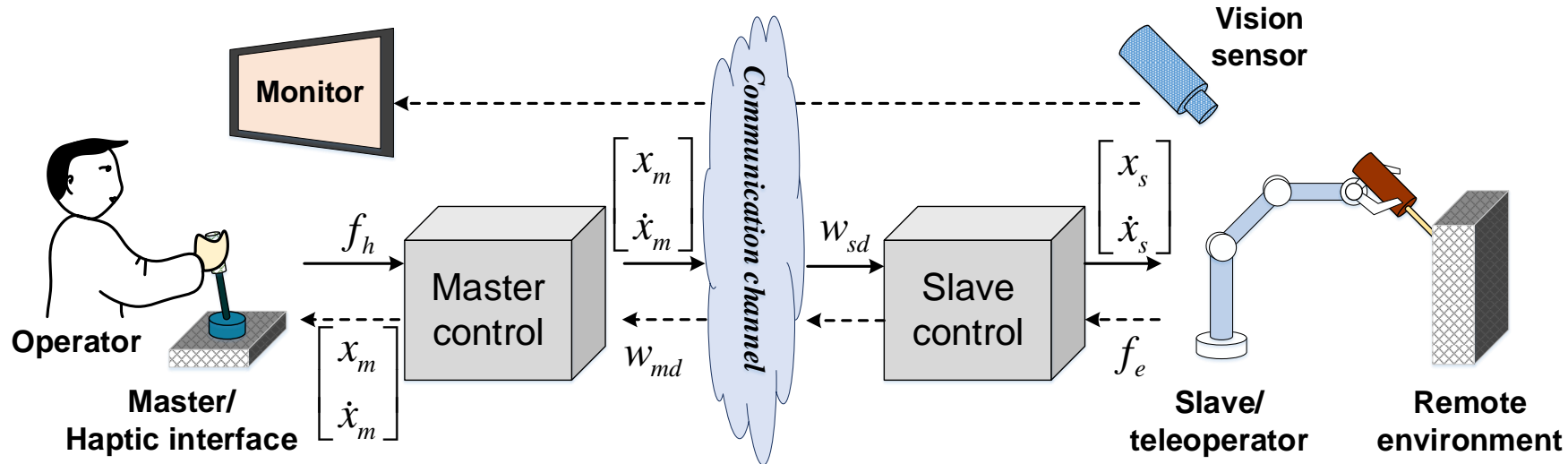


Figure 1.1. The bilateral haptic teleoperation architecture.



Robustness
Performance
Perception
Transparency
...

The **main** purpose is to provide technical means to **successfully perform a desired task** in the environment. (achieved a **high task performance**).
For evaluation, physically accessible quantities (task completion time, measurement error, applied forces or dissipated energies)

Overview of the BHTS structure

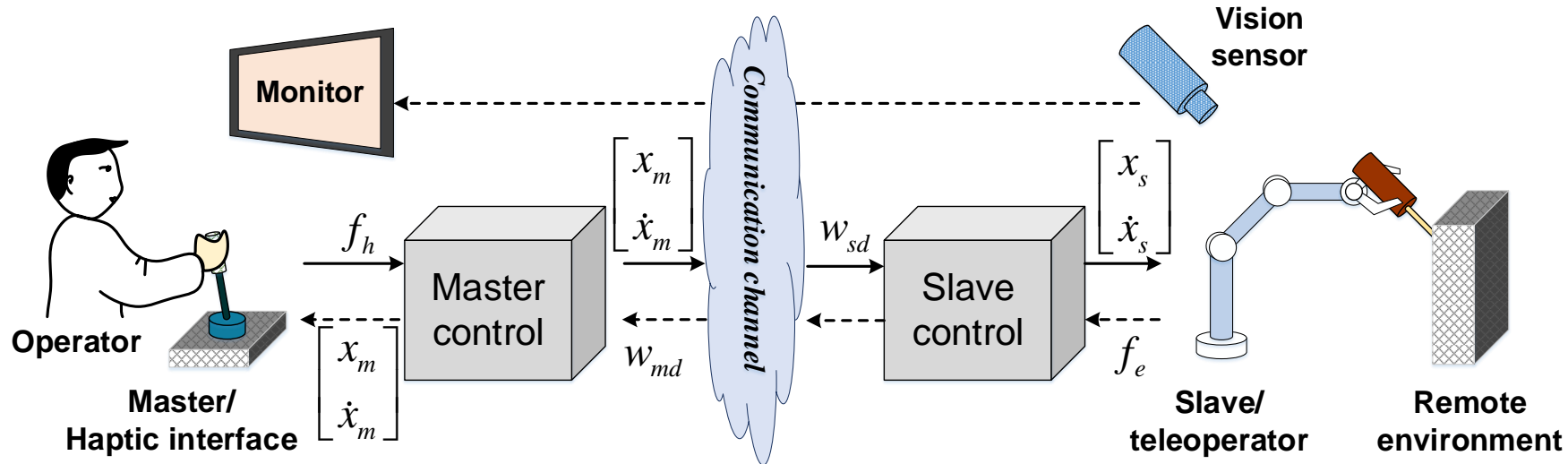


Figure 1.1. The bilateral haptic teleoperation architecture.

Robustness
 Performance
 Perception
 Transparency
 ...

It refers to the operator's **feeling of being there**. Ideally, the operator **can distinguish** a remote environment, that presence is **correlated** with task performance in a positive, causal way. It implies that by improving the feeling of presence task performance is improved as well.

Overview of the BHTS structure

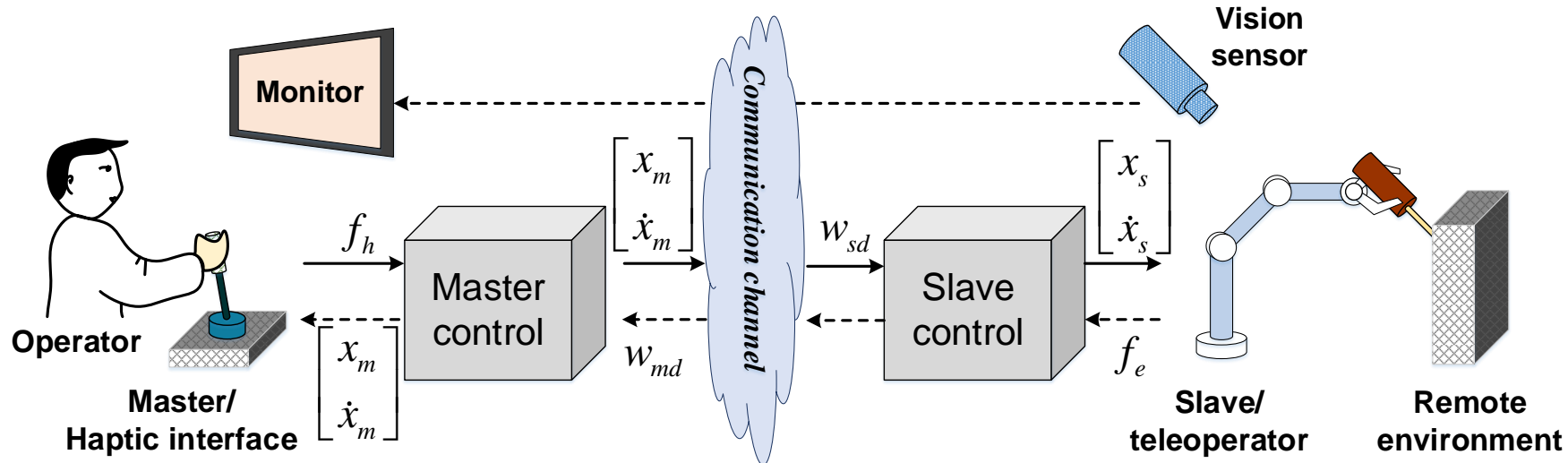


Figure 1.1. The bilateral haptic teleoperation architecture.

Robustness
Performance
Perception
Transparency
 ...

Compared to **perception**, it is a quantitative objective. Transparency and **robustness** are conflicting objectives, (**trade-off**). A measure for transparency is **fidelity**. It describes the ability to exactly display the environment to the operator.

Overview of the BHTS structure

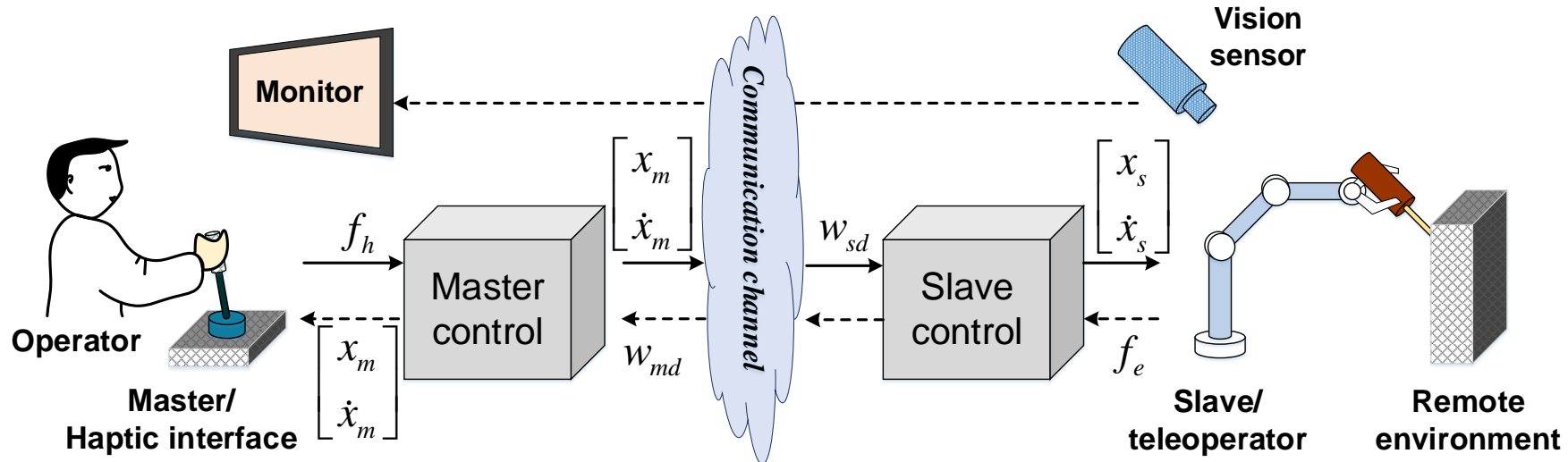


Figure 1.1. The bilateral haptic teleoperation architecture.

evaluate

Robustness
Performance
Perception
Transparency

achieve

Variable Impedance Control [5, 6]
Model-mediated Teleoperation [40]
Movement Estimation [78, 79]
Passivity [27], Prediction [39], ...

classify

Environment condition
Operator's characteristics
Communication channel

1. INTRODUCTION

✓ PAM actuator

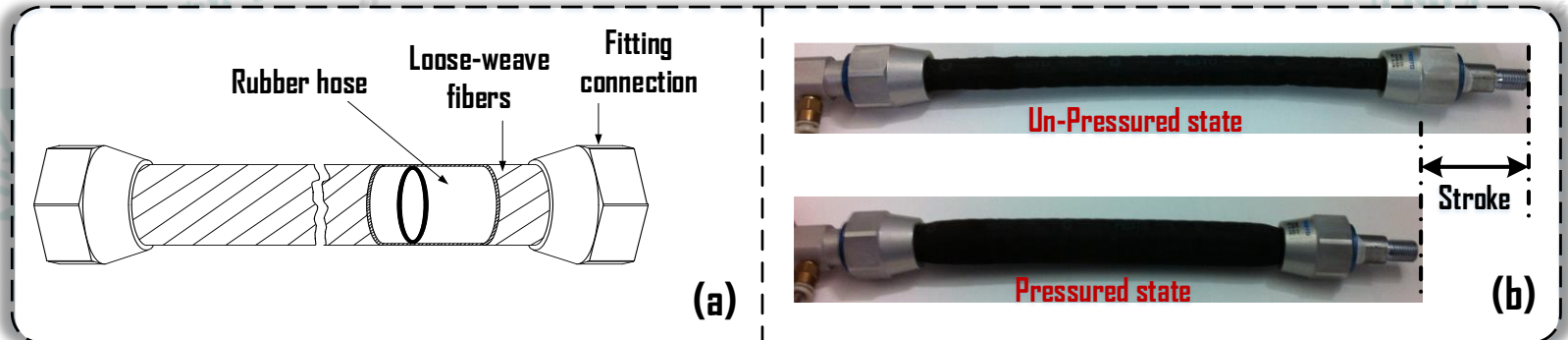
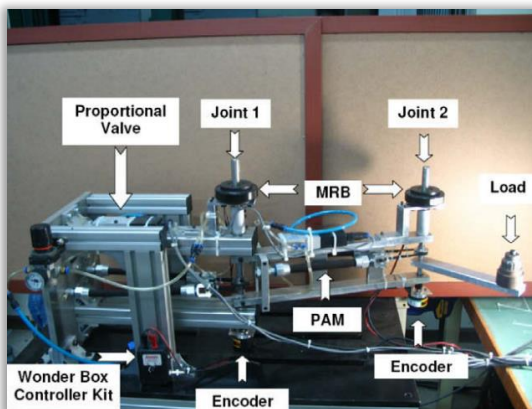
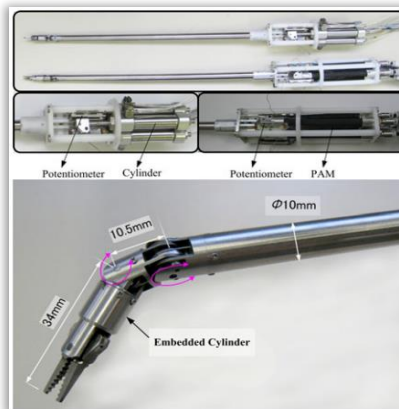


Fig. 1.2. (a) Structure and (b) working principle of the PAM.



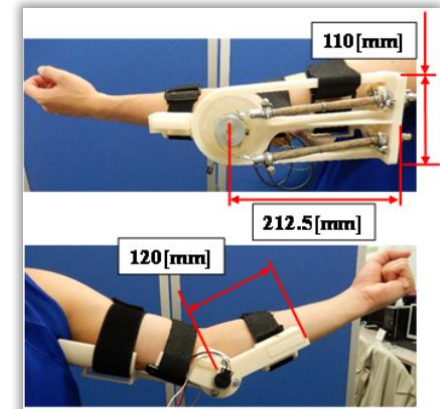
2-joint manipulator [16, 17]



Forceps' manipulators [20]



KNEXO robot [22]



Wearable Haptic Device [23]

Research Objectives

01 Propose Position Tracking Controller

An integral terminal-style SMC is designed with the combination of an adaptive gain and TDE technique

03 Propose Model-free Control for slave-environment interaction

Applying RL approximation method to learning the optimal contact force (minimal) online

05 Propose Force Sensorless reflecting control for bilateral haptic teleoperation

The new AFOB is proposed to estimate the force signals. Achieving great transparency (position, force feedback)

02 Propose Finite-Time Force Controller

An adaptive gain Fast ITSMC-TDE scheme is established with a friction-free disturbance technique in finite-time

04 Propose optimal impedance for human-master interaction

Using IRL to optimize the prescribed impedance model parameters to assist minimum human effort



1

Introduction

2

Modeling and platform setup based on the APAM configuration

3

Adaptive Gain ITSMC with TDE scheme

4

Adaptive Finite-Time Force Sensorless Control scheme with TDE

5

Model-free control for Optimal contact force in Unknown Environment

6

Optimized Human-Robot Interaction control using IRL

7

Force Sensorless Reflecting Control for BHTS

8

Conclusion and Future works

2. MODELING AND PLATFORM SETUP BASED ON THE APAM CONFIGURATION

Mathematical modeling

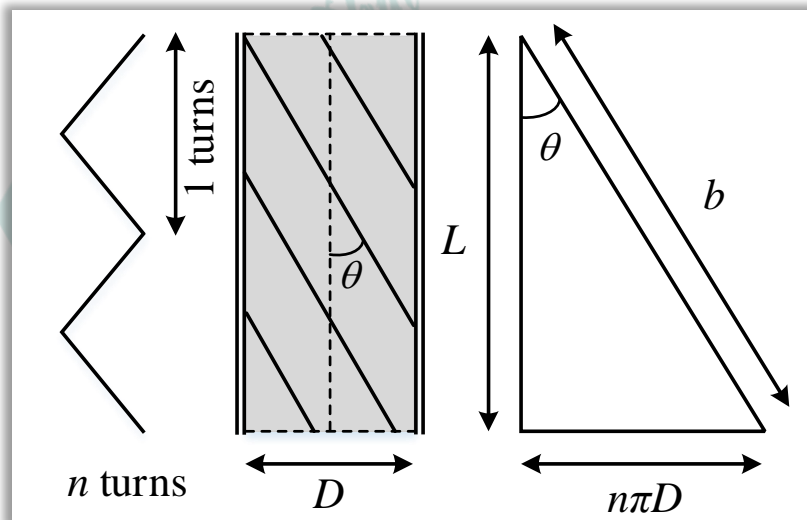


Fig. 2.1. A cross-sectional view of the simplified geometric model.

Table 2.1. Parameters of the studied PAM

Parameter	Description	Value	Unit
P_s	Supply pressure	6.5	bar
B	Viscous damping coefficient	50	N.s/mm
M	Mass of the plate	0.5	Kg
L_0	Original length of the PAM	175	mm
n	Number of turns of the thread	1.04	
b	Thread length	200	mm

The tensile force of each PAM [7]:

$$F = -P \frac{dV}{dL} = -P \frac{dV/d\theta}{dL/d\theta} = -P \frac{b^2 - 3L^2}{4\pi n^2}$$

The motion equation of the system:

$$M\ddot{x} + B\dot{x} = F_1 - F_2 + \Delta$$

The motion equation of the system:

$$\ddot{x} = f_0(x, \dot{x}) + g_0(x)u + d$$

$$\begin{cases} f(x) = -\frac{3P_0L_0x}{\pi n^2 M} - \frac{B\dot{x}}{M}; & g(x) = \frac{3(L_0^2 + x^2) - b^2}{2\pi n^2 M} \\ d = (f(x, \dot{x}) - f_0(x, \dot{x})) + (g(x) - g_0(x))u + \Delta \end{cases}$$

where $f_0(x)$, $g_0(x)$ are the nominal value of $f(x)$, $g(x)$. d is a total of unknown disturbances.

2. MODELING AND PLATFORM SETUP BASED ON THE APAM CONFIGURATION

Experimental modeling

The approximated PAM model based on its pressure and contraction strain:

$$M_k \ddot{\xi}_k + b_k(P_k) \dot{\xi}_k + k_k(P_k) \xi_k = f_k(P_k)$$

$$\begin{cases} b_k(P_k) = b_{k1}P_k + b_{k0} \\ k_k(P_k) = k_{k1}P_k + k_{k0} \quad (k = 1, 2) \\ f_k(P_k) = f_{k1}P_k + f_{k0} \end{cases}$$

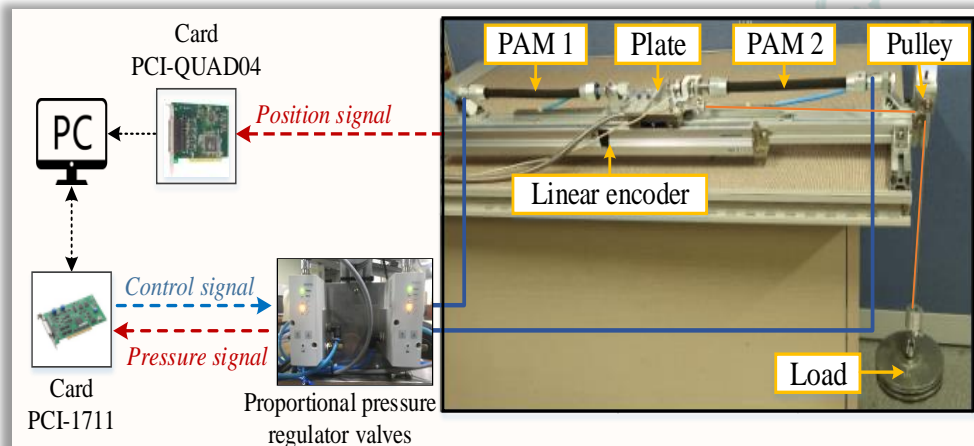


Fig. 2.2. Block diagram of the experimental system

Table 2.2. List of APAM model parameters.

	Parameter	Value	Units
Spring elements	k_{k1}	117.32	N/m/bar
	k_{k0}	6.8	N/m
Damping elements	b_{k1}	96.2	N/m/s/bar
	b_{k0}	0.85	N/m/s
Force elements	f_{k1}	91.22	N/bar
	f_{k0}	4.73	N

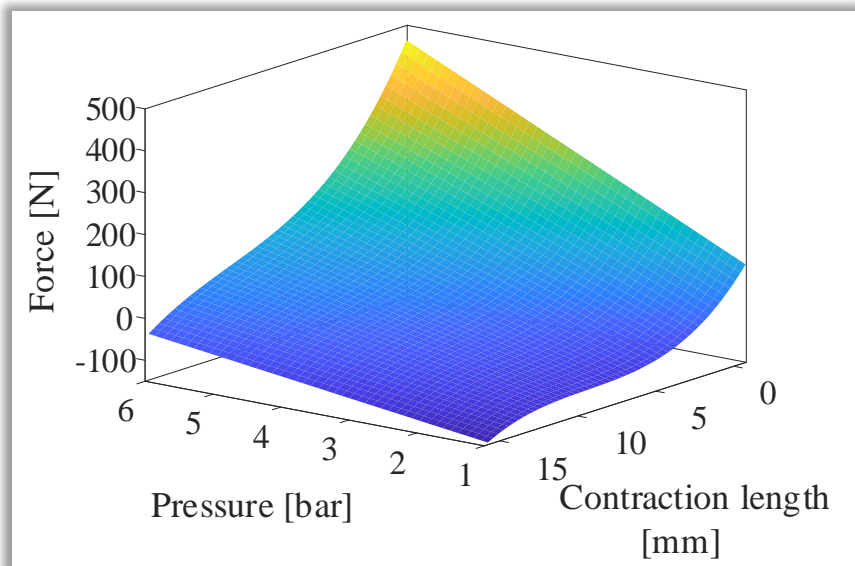
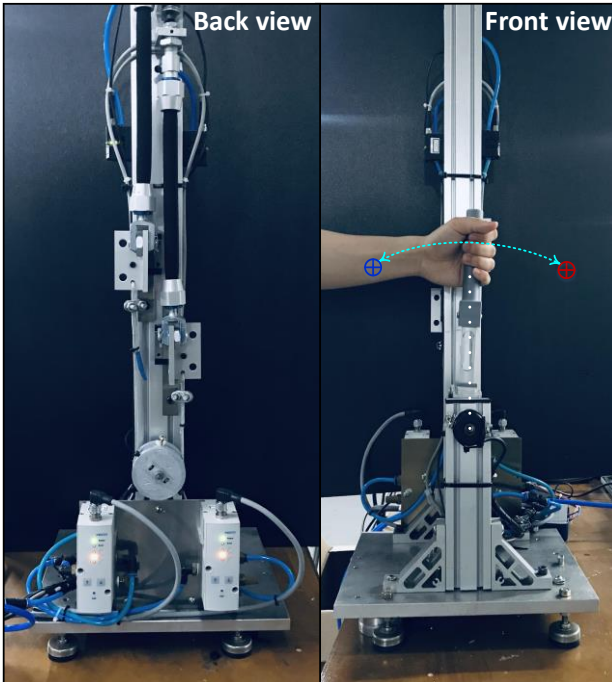
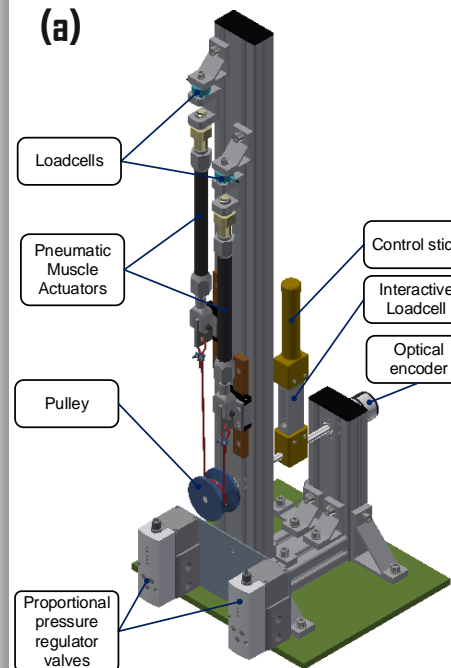


Fig. 2.3. Experimental model for certain separate pressure.

2. MODELING AND PLATFORM SETUP BASED ON THE APAM CONFIGURATION

Platform setup

(a)



(b)

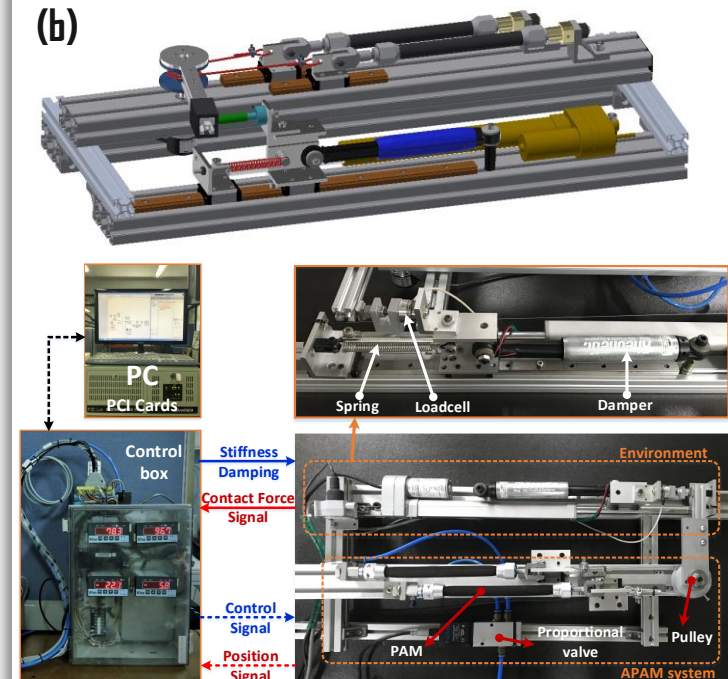


Fig. 2.5. The APAM-based (a) master and (b) slave subsystem configuration.

2. MODELING OF THE BILATERAL TELEOPERATION SYSTEM

Platform setup

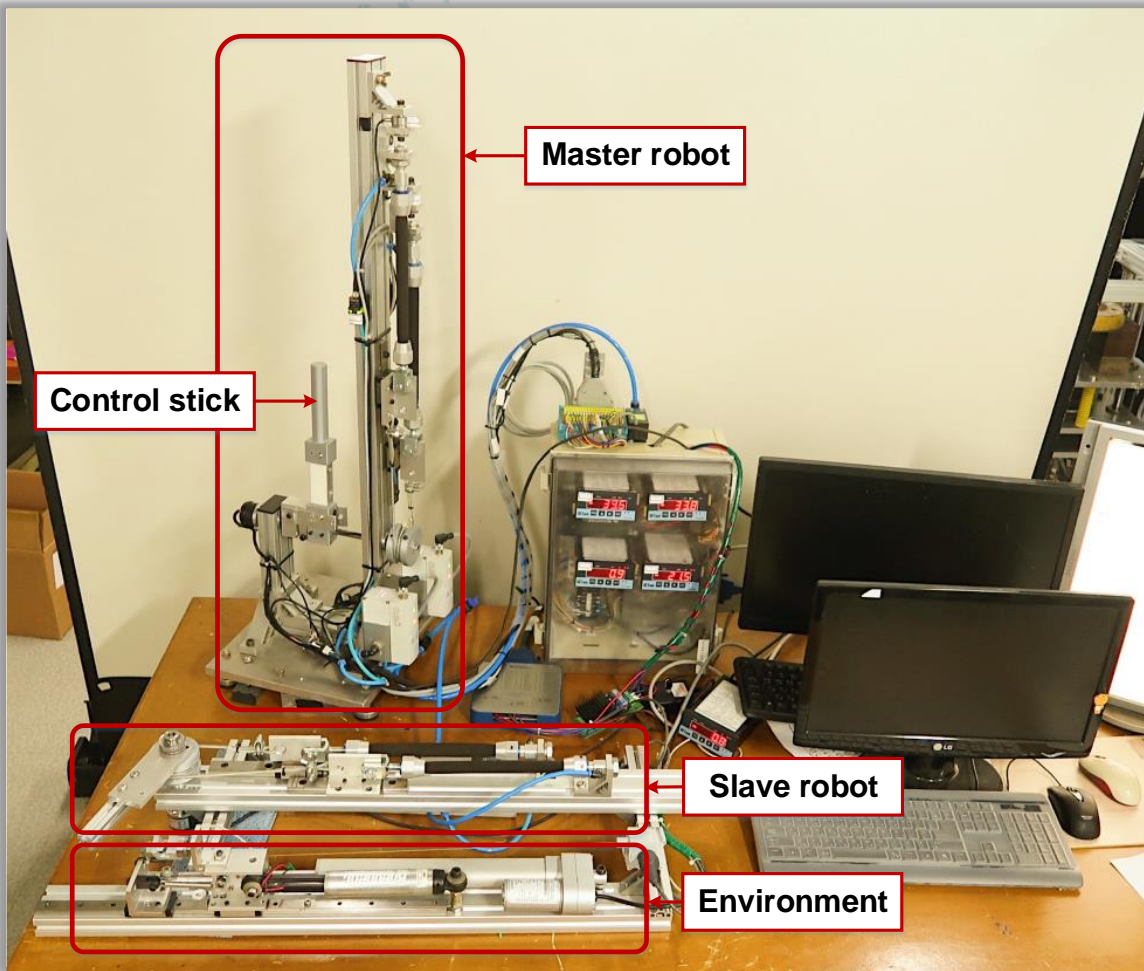


Table 2.3. Specifications of the exp. devices

Device	Description
PAM	Festo MAS-10-200N-AA-MC-0
	Nominal length: 200 mm
	Inside diameter: 10 mm
	Max pressure: 8 bar
PPR Valve	Festo VPPM-8L-L-1-G14-DL8H
	Max pressure: 8 bar
DAQ Card	ADVANTECH PCI-1711
	AI/AO: 12 bits (resolution)
Linear encoder	MEASUREMENT PCI-QUAD04
	Type: Rational WTB5-0500MM
	Resolution: 0.005 mm

Fig. 2.6. Photograph of the experimental apparatus of the overview BHTS.

1

Introduction

2

Modeling and platform setup based on the APAM configuration

3

Adaptive Gain ITSMC with TDE scheme for the position control

4

Adaptive Finite-Time Force Sensorless Control scheme

5

Model-free control for Optimal contact force in Unknown Environment

6

Optimized Human-Robot Interaction force control using IRL

7

Force Sensorless Reflecting Control for BHTS

8

Conclusion and Future works

3. AN ADAPTIVE GAIN ITSMC-TDE SCHEME FOR THE POSITION CONTROL

Proposed control idea

3

The control effectiveness is verified by experimental trials in different challenging work conditions (compare several controllers)

2

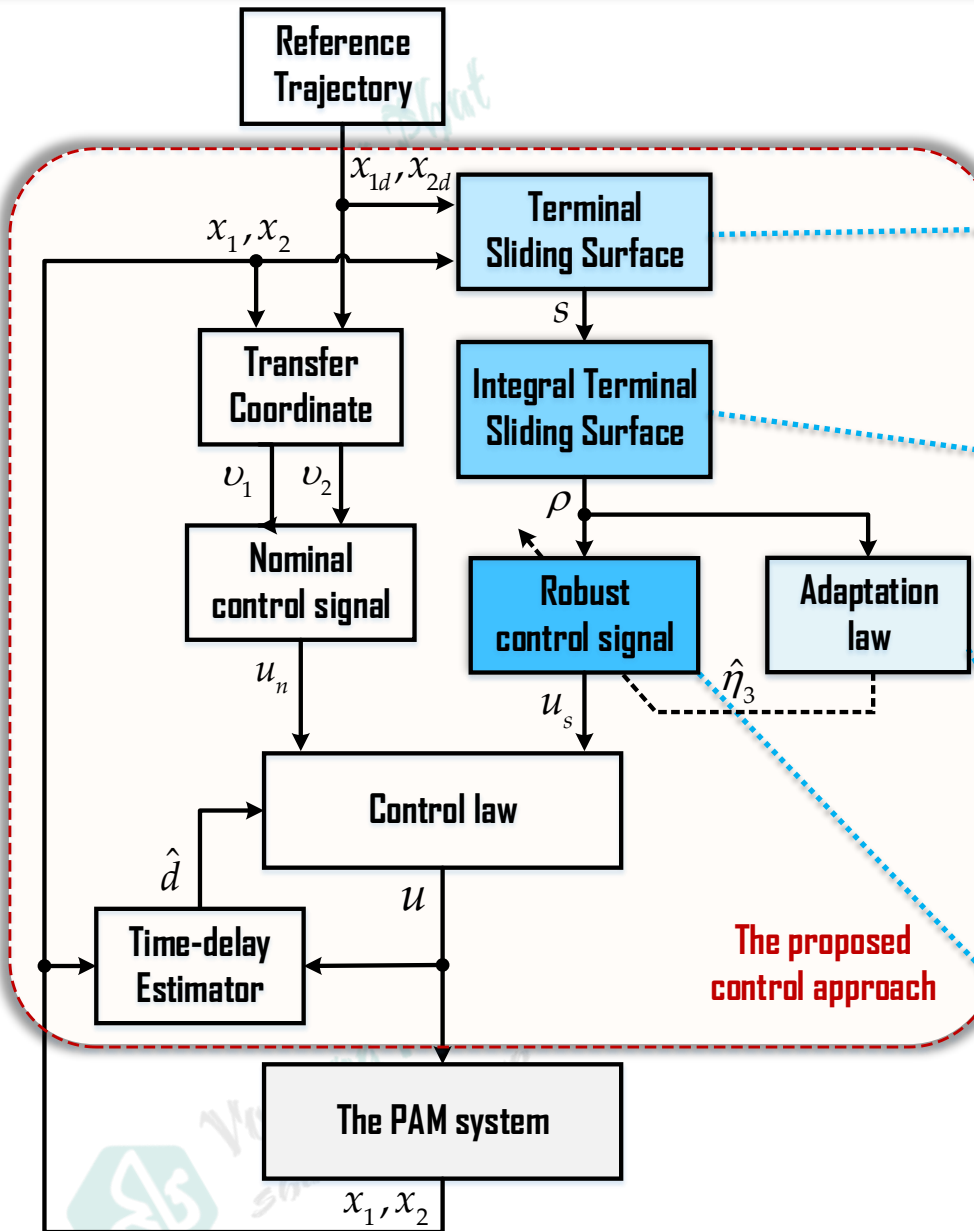
The stability of the controlled system is theoretically analyzed

1

The first time the AITSMC-TDE scheme is proposed for a PAM system



3. AN ADAPTIVE GAIN ITSMC-TDE SCHEME FOR THE POSITION CONTROL



Control design

A terminal sliding surface is chosen:

$$s = e_2 + k_1 e_1 + k_2 e_1^\alpha$$

A proposed integral sliding surface is designed:

$$\rho = s(t) - s(t_0) - \int_{t_0}^t (k_1 e_2 + \alpha k_2 e_1^{\alpha-1} e_2 + f_0(x_1, x_2) + g_0(x_1) u_n - \ddot{x}_{1d}) d\tau$$

An adaptive law for the robust gain:

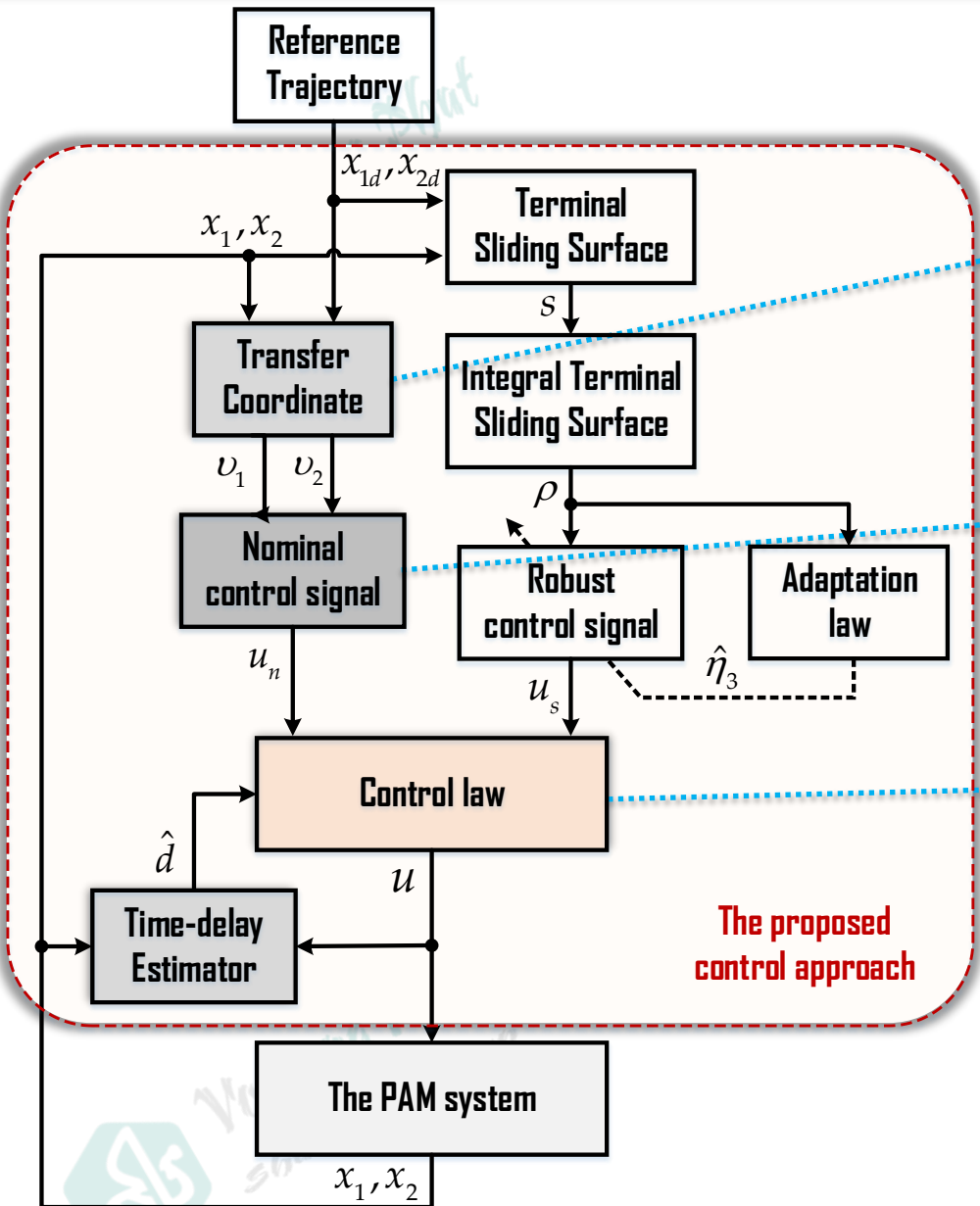
$$\dot{\hat{\eta}}_3 = \frac{1}{\mu} |\rho(t)| \quad \text{or} \quad \begin{cases} \hat{\eta}_3(t) = \hat{\eta}_3(t_m) |\chi| + \eta_0 \\ \sigma \dot{\chi} + \chi = \text{sign}(\rho(t)) \end{cases}$$

A robust control signal can be redesigned:

$$u_s(t) = -(g_0(x_1))^{-1} [\hat{\eta}_3 \text{sign}(\rho) + \kappa_3 \rho + \kappa_4 \rho^{\gamma_3}]$$

Proof: See more detail in Appendix 3.2, 3.3

3. AN ADAPTIVE GAIN ITSMC-TDE SCHEME FOR THE POSITION CONTROL



Control design

The auxiliary variables are defined:

$$\begin{cases} \nu_1 = e_1 = x_1 - x_{1d} \\ \nu_2 = x_2 - \beta_1 \end{cases}$$

The nominal control signal can be designed as

$$u_n = (g_0(x_1))^{-1} [\ddot{x}_{1d} - \nu_1 - f_0(x_1, x_2) - \eta_1 \dot{\nu}_1 - \kappa_1 \nu_1^{\gamma_1-1} \dot{\nu}_1 - \eta_2 \nu_2 - \kappa_2 \nu_2^{\gamma_2}]$$

The control law can be rewritten:

$$u(t) = u_n + u_s - g(x_1)^{-1} \hat{d}$$

where

$$\begin{aligned} \hat{d} = & \dot{x}_2(t-t_d) - f_0(x_1(t-t_d), x_2(t-t_d)) \\ & - g_0(x_1(t-t_d)) u(t-t_d) \end{aligned}$$

Proof: See more detail in Appendix 3.1, 3.4-3.5

3. AN ADAPTIVE GAIN ITSMC-TDE SCHEME FOR THE POSITION CONTROL



Experimental validation

Case study 1 (no load): $x_d \text{ (mm)} = 8 * \sin(0.4\pi t)$

Case study 2 (no load): $x_d \text{ (mm)} = 8 * \sin(\pi t)$

Case study 3 (no load): A multistep trajectory

Case study 4 (with load): $x_d \text{ (mm)} = 8 * \sin(\pi t)$
in turn, 2-kg-load and 7-kg-load



Parameters

PID control:

for case study 3: $K_P = 1.5, K_I = 18, K_D = 0.05$

for other case: $K_P = 3.5, K_I = 28, K_D = 0.1$;

Proposed control:

for ITSMC, $\eta_1 = 3, \eta_2 = 1.5, \eta_3 = 2.5, \kappa_1 = \kappa_3 = 10, \kappa_2 = \kappa_4 = 2, \gamma_1 = \gamma_2 = 5/7, k_1 = 2, k_2 = 5.5, \alpha = 9/11$;
for adaptative gain, $\mu = 10, \delta = 0.05, \sigma = 0.1$.

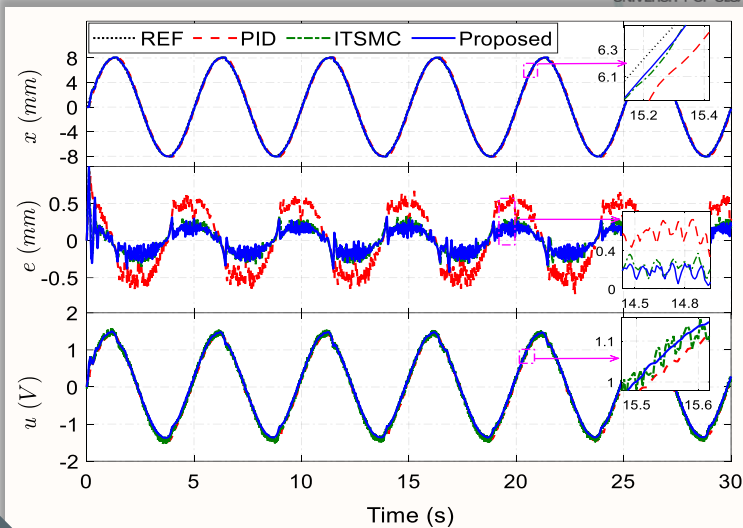


Fig. 3.1. Performance response in case study 1.

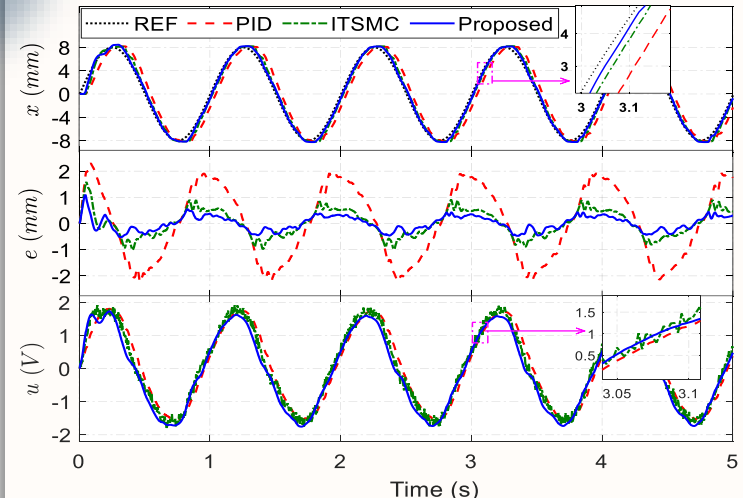


Fig. 3.2. Performance response in case study 2.

3. AN ADAPTIVE GAIN ITSMC-TDE SCHEME FOR THE POSITION CONTROL



Experimental validation

Case study 1 (no load): $x_d \text{ (mm)} = 8 * \sin(0.4\pi t)$

Case study 2 (no load): $x_d \text{ (mm)} = 8 * \sin(\pi t)$

Case study 3 (no load): A multistep trajectory

Case study 4 (with load): $x_d \text{ (mm)} = 8 * \sin(\pi t)$
in turn, 2-kg-load and 7-kg-load

Table 3.1. A quantitative comparison between the tracking performances.

Controller		PID	ITSMC	Proposed
Sine 0.2 Hz - 8 mm	$L_2[e]$	0.4102	0.1737	0.1574
	$L_2[u]$	0.9961	1.0270	0.9602
Sine 1 Hz - 8 mm	$L_2[e]$	1.1845	0.4996	0.3788
	$L_2[u]$	1.1284	1.1152	1.0900
Multistep	$L_2[e]$	0.8587	0.6846	0.6368
	$L_2[u]$	0.7670	0.7333	0.7247
Sine 1 Hz - 8 mm with 2-kg-load	$L_2[e]$	1.2578	0.8314	0.4779
	$L_2[u]$	1.1414	1.1506	1.1287
Sine 1 Hz - 8 mm with 7-kg-load	$L_2[e]$	1.5937	1.0827	0.5067
	$L_2[u]$	1.1613	1.1729	1.1584

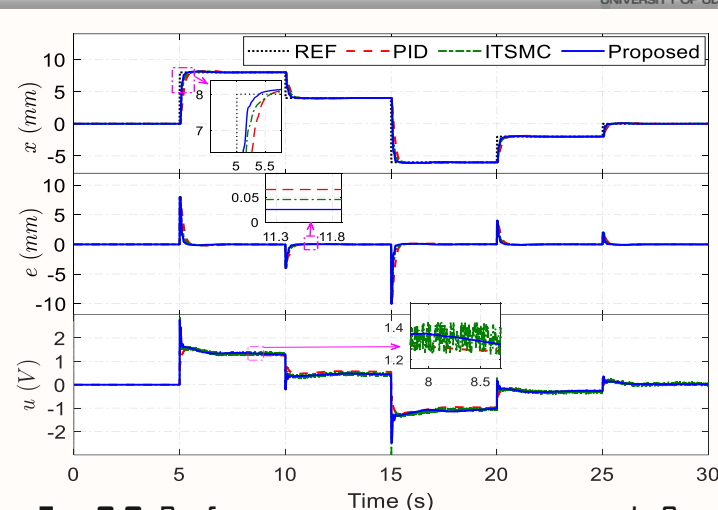


Fig. 3.3. Performance response in case study 3.

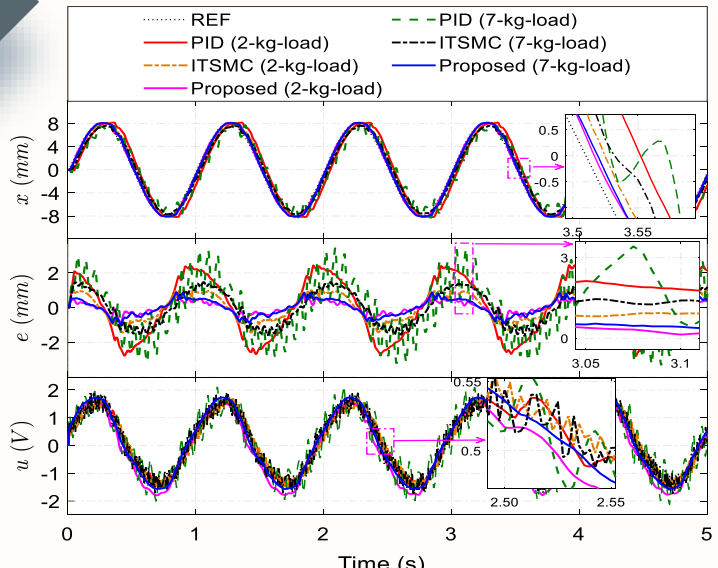
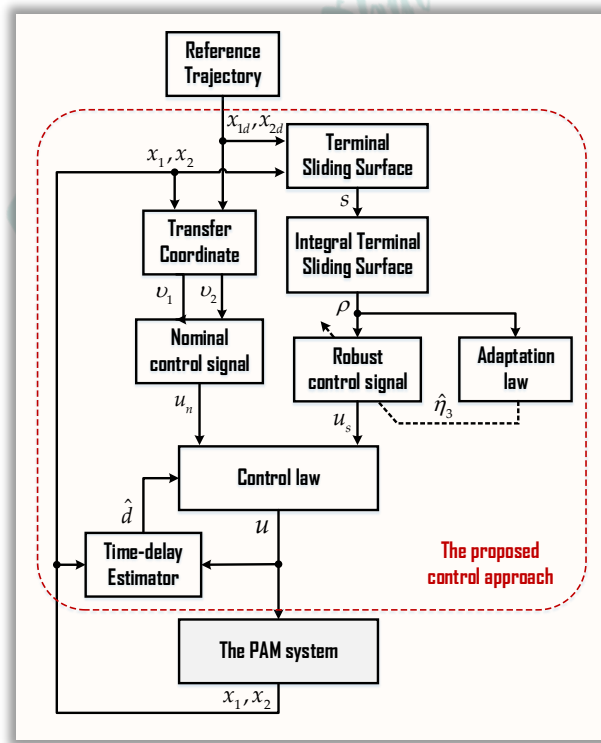


Fig. 3.4. Performance response in case study 4.

3. AN ADAPTIVE GAIN ITSMC-TDE SCHEME FOR THE POSITION CONTROL

Summary



Robust performance against uncertainties and disturbances

Finite-time convergence of the tracking errors

Reducing the chattering phenomenon

Eliminating the reaching phase

Fast transient response

Next works will be directed to the control using the **force properties**.

1

Introduction

2

Modeling and platform setup based on the APAM configuration

3

Adaptive Gain ITSMC with TDE scheme

4

Adaptive Finite-Time Force Sensorless Control scheme

5

Model-free control for Optimal contact force in Unknown Environment

6

Optimized Human-Robot Interaction force control using IRL

7

Force Sensorless Reflecting Control for BHTS

8

Conclusion and Future works

Proposed control idea



The proposed FSOB scheme obtains force information, eliminated noise and static friction

The FITSMC guarantees the finite convergence; new adaptive gain and TDE are deployed to handle online (uncertainties and chattering phenomenon)

Verified the reliability and superiority of the proposed control, demonstrated in different challenging work conditions



4. ADAPTIVE FINITE-TIME FORCE SENSORLESS CONTROL SCHEME

Control design

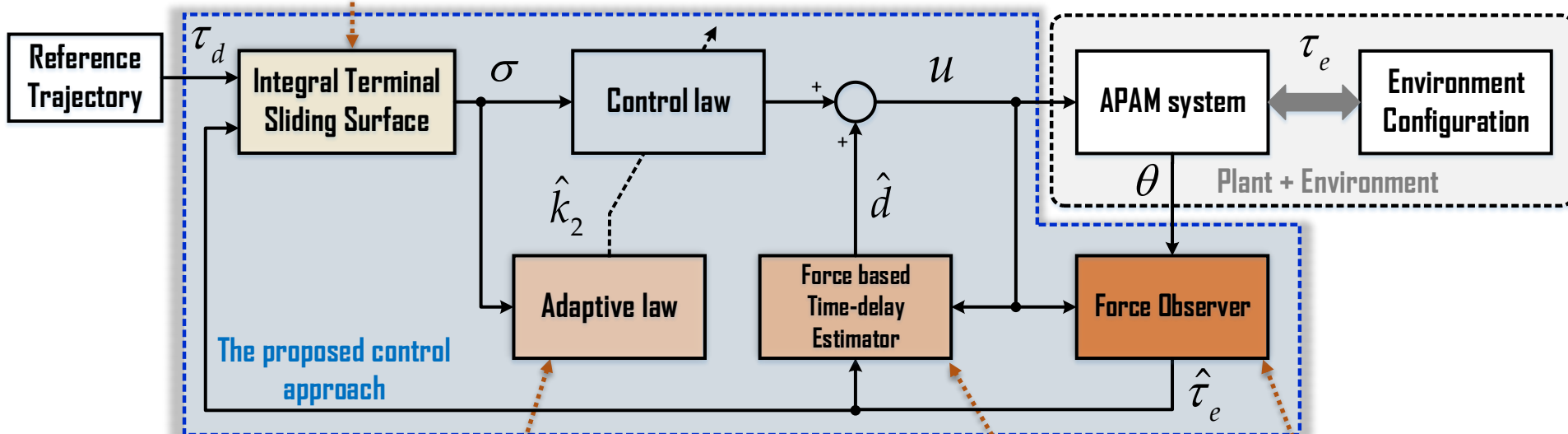
The FITSM surface is defined:

$$\sigma = e_f + \lambda_1 \int_0^t (e_f(\chi) + \lambda_2 \text{sign}(e_f(\chi))^{[v]}) d\chi$$

The control law can be rewritten:

$$u(t) = \hat{d}(t) + K_c^{-1} \left[\tau_d + \lambda_1^{-1} \dot{e}_f + \lambda_2 \text{sign}(e_f)^{[v]} + \kappa_4 \sigma + \hat{\kappa}_5 \text{sign}(\sigma)^{[v]} \right]$$

Proof: See in Appendix 4.1 – 4.3



An adaptive switching gain law:

$$\dot{\kappa}_5 = \frac{\eta_5}{\eta_4^{\text{sign}(|\sigma| - \varepsilon_\sigma)}} |\sigma|^{[v+1]} \text{sign}(|\sigma| - \varepsilon_\sigma)$$

An estimated lumped disturbance:

$$\hat{d}(t) \cong d(t - t_d) = u(t - t_d) - \hat{K}_c^{-1} \hat{\tau}_e(t - t_d)$$

Force observer based-Led [40]:

$$\hat{\tau}_e = \frac{\hat{\tau}_e^* + 2\xi_e \omega_e \hat{\tau}_e^* + \omega_e^2 \hat{\tau}_e^*}{\omega_e^2}$$

4. ADAPTIVE FINITE-TIME FORCE SENSORLESS CONTROL SCHEME



Experimental validation

Scenario 1: $\tau_d(N) = 75 \cdot \sin(0.2\pi t - \pi/2) + 62.5$

Scenario 2: $\tau_d(N) = 75 \cdot \sin(0.8\pi t - \pi/2) + 62.5$

Scenario 3: A multistep trajectory with a LPF's bandwidth of 0.2(rad/s).



Parameters

Observers:

for FSQB: $\omega = 500$ rad/s; $\zeta = 0.001$, $\alpha_1 = 20$, $\alpha_2 = 12$,
 $\alpha_3 = 5$, $\alpha_4 = 1.5$.

Proposed control:

for ITSMC, $\eta_1 = 3$, $\eta_2 = 1.5$, $\eta_3 = 2.5$, $\kappa_1 = \kappa_3 = 10$,
 $\kappa_2 = \kappa_4 = 2$, $\gamma_1 = \gamma_2 = 5/7$, $k_1 = 2$, $k_2 = 5.5$, $v = 9/11$;
for adaptative gain, $\mu = 10$, $\delta = 0.05$, $\sigma = 0.1$.

PID control:

for case study 3: $K_P = 1.5$, $K_I = 18$, $K_D = 0.05$;
for other case: $K_P = 3.5$, $K_I = 28$, $K_D = 0.1$;

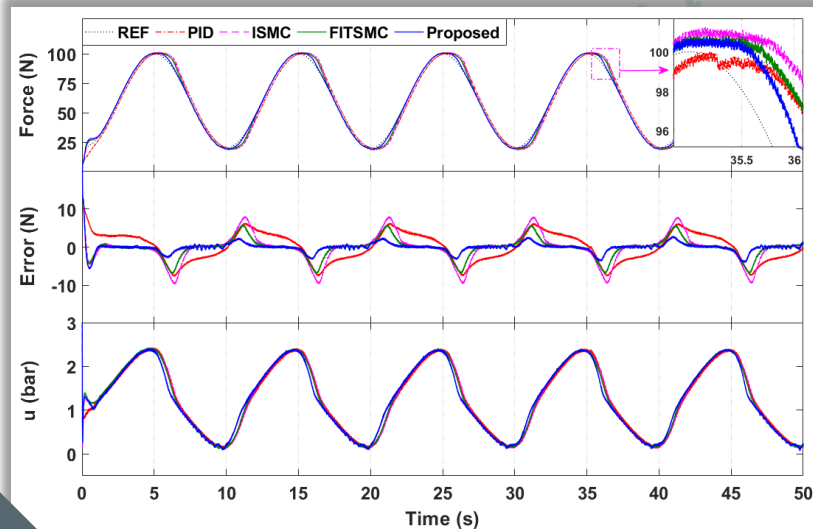


Fig. 4.2. Performance response in Scenario 1.

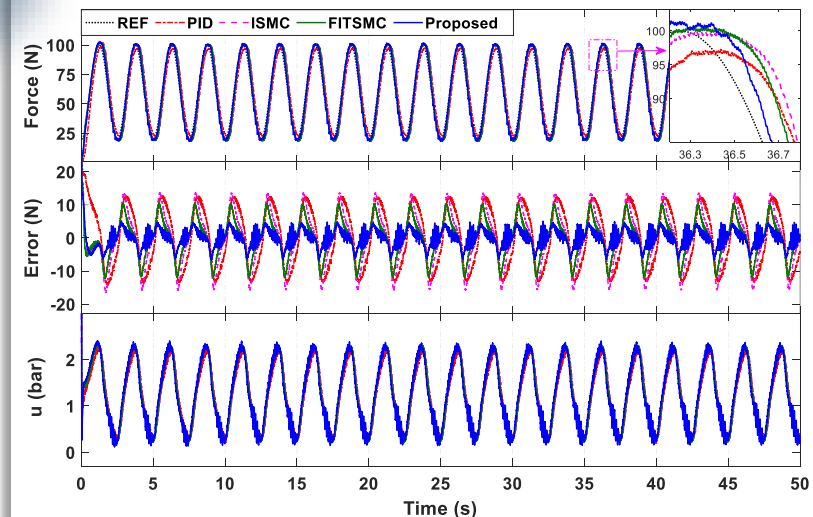


Fig. 4.2. Performance response in Scenario 2.

4. ADAPTIVE FINITE-TIME FORCE SENSORLESS CONTROL SCHEME



Experimental validation

Table 4.1. A RMSE comparison between the tracking error performances.

Controller	PID	ISMC	FITSMC-TDE	Proposed
Sine 0.1 Hz	2.1050	1.2152	0.9440	0.5158
Sine 0.4 Hz	3.2054	1.8045	2.0632	1.9807
Multistep	2.6508	2.3548	2.0618	1.7685

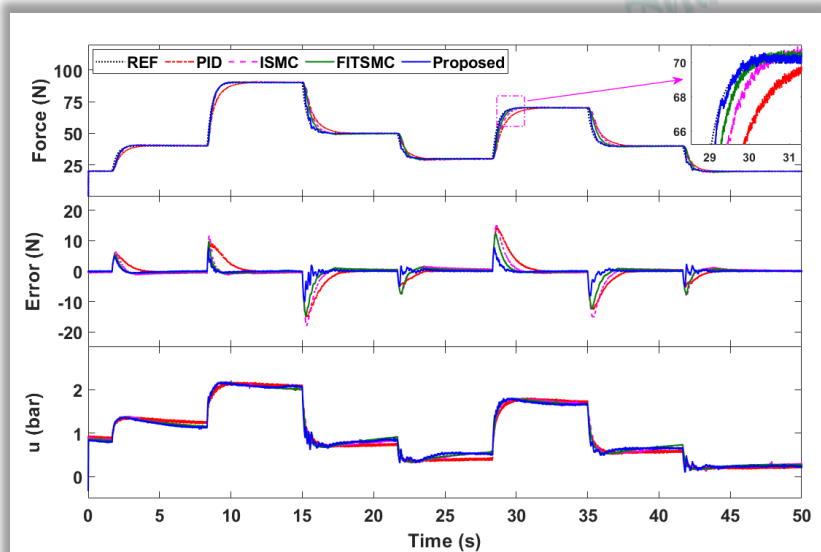


Fig. 4.3. Performance response in Scenario 3.



Discussion

- Improved the control performances (fast response, high accuracy, and robustness)
- Guaranteed the finite convergence
- Cancelling the lumped uncertainties via TDE solution and the switching gain in the FITSMC online

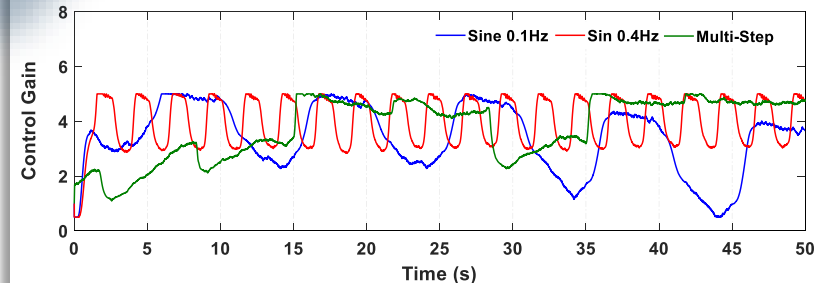


Fig. 4.4. Control gain.

1

Introduction

2

Modeling and platform setup based on the APAM configuration

3

Adaptive Gain ITSMC with TDE scheme

4

Adaptive Finite-Time Force Sensorless Control scheme

5

Model-free control for Optimal contact force in Unknown Environment

6

Optimized Human-Robot Interaction force control using IRL

7

Force Sensorless Reflecting Control for BHTS

8

Conclusion and Future works

Proposed control idea



1 The RL method is used to learn on-line the optimal desired force

2 The stability of the closed-loop control is theoretically demonstrated by the Lyapunov approach

3 Verified effective for robot interaction control in unknown environments



Control design

The force control

$$x_f(s) = K_{Pf}e_f(t) + K_{If} \int_t^{\infty} e_f(\tau)d\tau$$

The environment is modeled as a spring-damper system [81]

$$F_e(t) = -C_e \dot{x}(t) + K_e(x_e - x(t))$$

The optimal impedance model

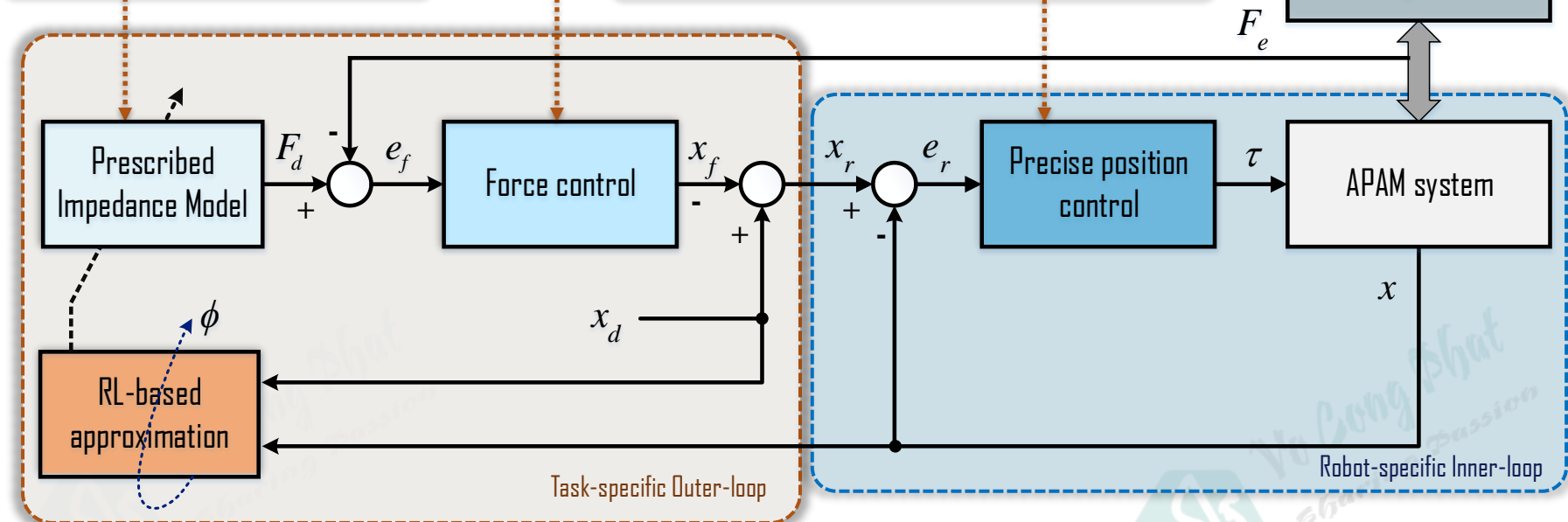
$$\dot{e}_r(t) = Ae_r(t) + BF_d(t)$$

$$Z(e_r(t)) = F_d^*(t)$$

The position control in task space

$$\begin{aligned} \tau = & \bar{M}\ddot{e}_r(t) + \bar{C}\dot{e}_r(t) + \bar{K}e_r(t) \\ & - \varepsilon sign(\sigma) - \rho_1\sigma - \rho_2\sigma^{[v]} + F_e(t) \end{aligned}$$

Environment Configuration





Implementation procedure

The main objective of this work is to determine the optimal desired force F_d^* , which is the minimum force that minimizes the position error e_r

$$F_d^*(t) = \kappa_e e_r(t)$$

LQR solution

RL solution

IRL approximation



The discounted cost function

$$J_s(e_r(t), F_d) = \int_t^\infty \gamma(\tau - t) \left(e_r^T(\tau) S e_r(\tau) + F_d^T(\tau) R F_d(\tau) \right) d\tau$$



The Algebraic Riccati equation

$$A^T P A + S + P + A^T P B \kappa_e = 0$$



The feedback control gain

$$\kappa_e = - \left(B^T P B + \gamma^{-1} R \right)^{-1} B^T P A$$



offline solution

Implementation procedure

The main objective of this work is to determine the optimal desired force F_d^* , which is the minimum force that minimizes the position error e_r

$$F_d^*(t) = \kappa_e e_r(t)$$

LQR solution

RL solution

IRL approximation

online soliton: using the off-policy RL to find the solution of the given new ARE

The discounted cost function

$$V_s(e_r(t)) = \int_t^\infty r(e_r(\tau), F_d(\tau)) e^{-\gamma(\tau-t)} d\tau$$

where $r(e_r(\tau), F_d(\tau)) = e_r^T(\tau) S e_r(\tau) + F_d^T(\tau) R F_d(\tau)$

The new Algebraic Riccati equation

$$e_r^T(t) \left(A^T P + PA + S - \gamma P \right) e_r(t) + 2e_r^T(t) P B F_d(t) + F_d^T(t) R F_d(t) = 0$$

The Hamilton-Jacobi-Bellman equation

$$\min_{F_d} \left\{ \dot{V}_s^*(e_r(t)) + r(t) - \int_t^\infty \frac{\partial}{\partial t} (r(\tau) e^{-\gamma(\tau-t)}) d\tau \right\} = 0$$

The optimal desired force

$$F_d^*(t) = -H_{22}^{-1} H_{21} e_r(t)$$

$$Q^*(e_r(t), F_d(t)) = V_s^*(e_r(t)) = X^T H X$$

impossible for all time

Implementation procedure

The main objective of this work is to determine the optimal desired force F_d^* , which is the minimum force that minimizes the position error e_r

$$F_d^*(t) = \kappa_e e_r(t)$$

LQR solution

RL solution

IRL approximation

Q -function update law based on IRL

$$\begin{aligned} Q(e_r(t), F_d(t)) &= \int_t^{t+\Delta t} r(\tau) e^{-\gamma(\tau-t)} d\tau \\ &\quad + e^{-\gamma\Delta t} Q(e_r(t + \Delta t), F_d(t + \Delta t)) \end{aligned}$$

The reward function of the utility function

$$r(t) = e_r^T(t) S e_r(t) + F_d^T(t) R F_d(t)$$

minimize temporal difference error

The approximator of the Q -value function

$$\hat{Q}((e_r, F_d), \phi) = \sum_{i=1}^N \psi_i(e_r, F_d) \phi_i$$

The parameter update law

$$\psi_i'(e_r, F_d) = \frac{\psi_i'(e_r, F_d)}{\sum_{i=1}^N \psi_i'(e_r, F_d)},$$

$$\psi_i'(e_r, F_d) = \exp\left(-\frac{1}{2} [e_r - c_i, F_d - c_i]^T \beta_i^{-1} [e_r - c_i, F_d - c_i]\right)$$

$$\dot{\phi}(t) = v(t) \zeta(t) \Delta(t)$$

$$\dot{\Delta}(t) = -\delta_\Delta \Delta(t) + \frac{1}{\Delta t} \times \frac{\partial \hat{Q}(e_r(t), F_d(t); \phi(t))}{\partial \phi(t)}$$



Validation results



Parameters

Environment:

$C_e = 0.5 \text{ N.s.mm}^{-1}$, $K_e = 2 \text{ N.mm}^{-1}$; $r_0 = 165 \text{ mm}$
 $x_d = 39.917 \text{ mm}$, $x_e = 35 \text{ mm}$

Position/Force control:

$K_{Pf} = 0.001$, $K_{If} = 0.02$, $\lambda = 0.2$, $\eta_\Delta = 0.1$. $\rho_1 = 0.5$,
 $\rho_2 = 20$, $v = 9/11$, $\alpha = 5/7$.

LQR solution:

$\kappa_e = 0.0025$, $S = 1$, $R = 10$, $T = 0.001$, $A = -4.006$,
 $B = -0.002$

RL approximation:

$v = 0.9$, $\gamma = 0.9$, $\delta_\Delta = 0.65$, $\varepsilon = 0.1$, $\varepsilon\text{-decay} = 0.99$,
 $K = 10$, $\beta = 0.1$

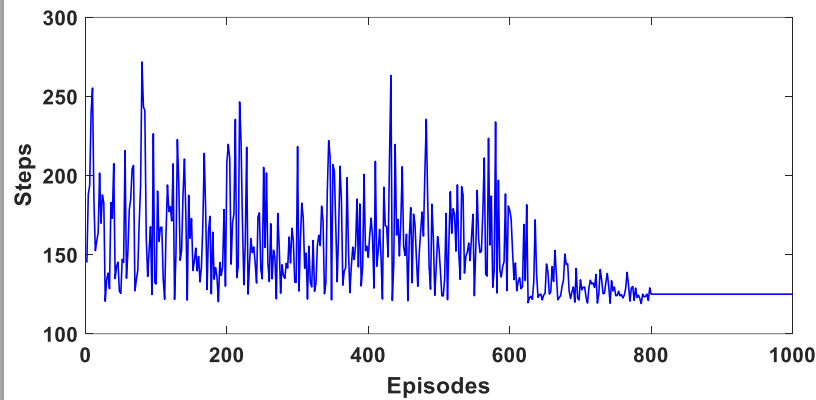


Fig. 5.1. RL in unknown environments during the learning process.

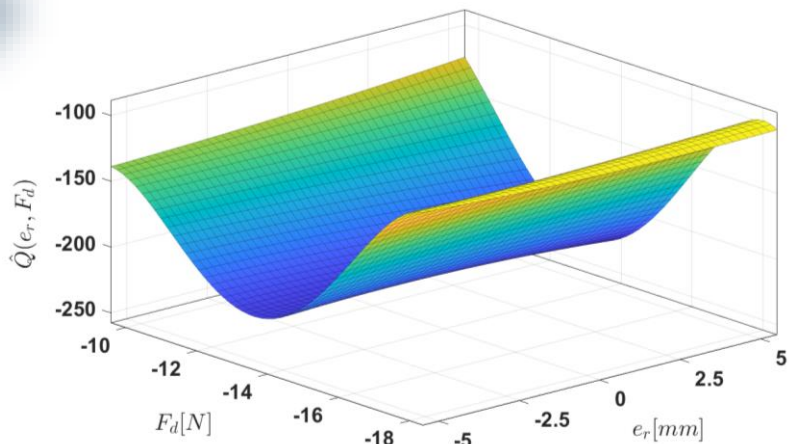


Fig. 5.2. Learning curves.



Validation results

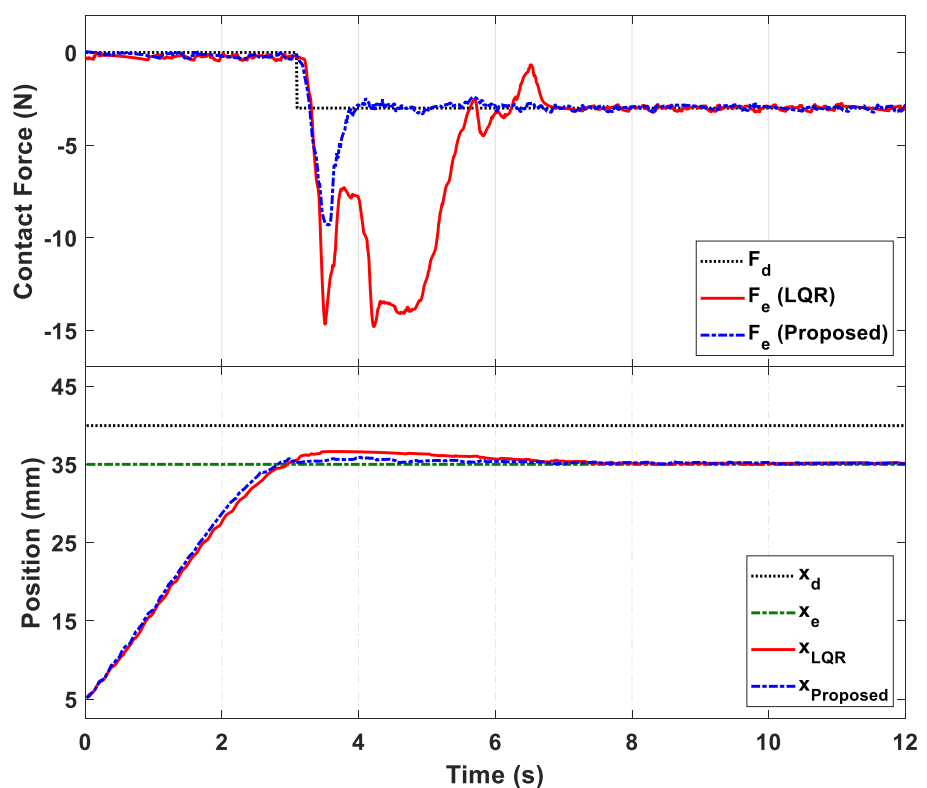


Fig. 5.3. Desired force/position tracking response

LQR solution

Three steps are required to complete the experiment:

- 1-the identification of the environment;
- 2-obtain the ARE solution using the environmental estimation
- 3-the complete experiment for the position/force controller.

IRL approximation

Achieving near-optimal performance without knowledge of the environment dynamics

C H A P T E R

1

Introduction

2

Modeling and platform setup based on the APAM configuration

3

Adaptive Gain ITSMC with TDE scheme

4

Adaptive Finite-Time Force Sensorless Control scheme

5

Model-free control for Optimal contact force in Unknown Environment

6

Optimized Human-Robot Interaction force control using IRL

7

Force Sensorless Reflecting Control for BHTS

8

Conclusion and Future works

Proposed control idea



The unknown human dynamics as well as the optimal overall human-robot system efficiency is verified in experimental trials.

The stability of the closed-loop control is theoretically demonstrated.



Find the optimal parameters of the impedance model to assure motion tracking and also assist the human with minimum effort to perform the task in real time.



6. OPTIMIZED HUMAN-ROBOT INTERACTION FORCE CONTROL USING IRL

Control design

The prescribed impedance model

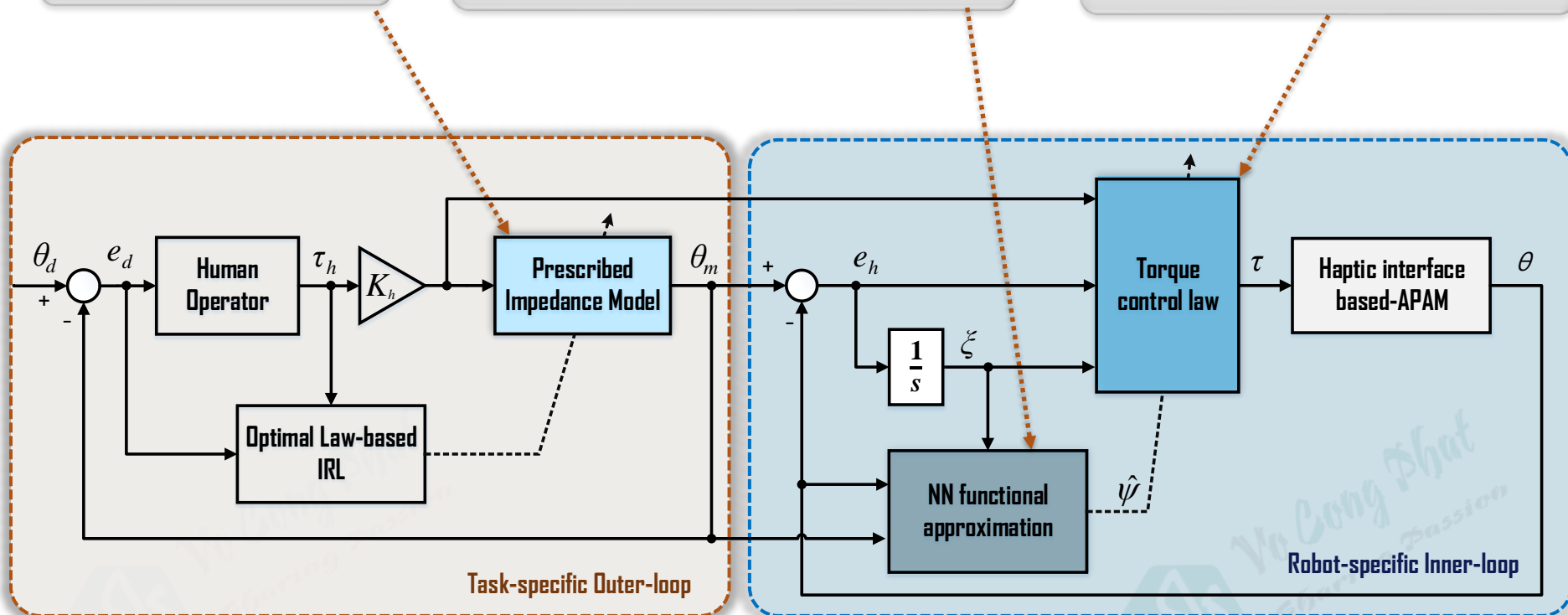
$$\theta_m = \frac{K_h \tau_h}{M_d s^2 + C_d s + K_d}$$

An approximation of the continuous function

$$\begin{aligned} \hat{\psi}(q) &= \hat{W}_1^T \phi(\hat{W}_2^T q) \\ \begin{cases} \dot{\hat{W}}_1 = F\hat{\phi}\sigma_h^T - F\hat{\phi}'\hat{W}_2^T q\sigma_h^T - kF\|\sigma_h\|\hat{W}_1 \\ \dot{\hat{W}}_2 = Gq(\hat{\phi}\hat{W}_1\sigma_h)^T - kG\|\sigma_h\|\hat{W}_2 \end{cases} \end{aligned}$$

The control torque in task space

$$\begin{aligned} \tau &= \hat{\psi} + K_s \left(\dot{e}_h + \mu_1 e_h + \mu_2 \int_0^t e_h(\tau) d\tau \right) \\ &\quad + K_q (\|\hat{Z}\| + Z_B) - K_h \tau_h \end{aligned}$$



6. OPTIMIZED HUMAN-ROBOT INTERACTION FORCE CONTROL USING IRL

Control design

The human transfer function

[99] Purpose: $\tau_h \rightarrow e_d$

$$G(s) = \frac{\kappa_p + \kappa_d s}{1 + k_e s}$$

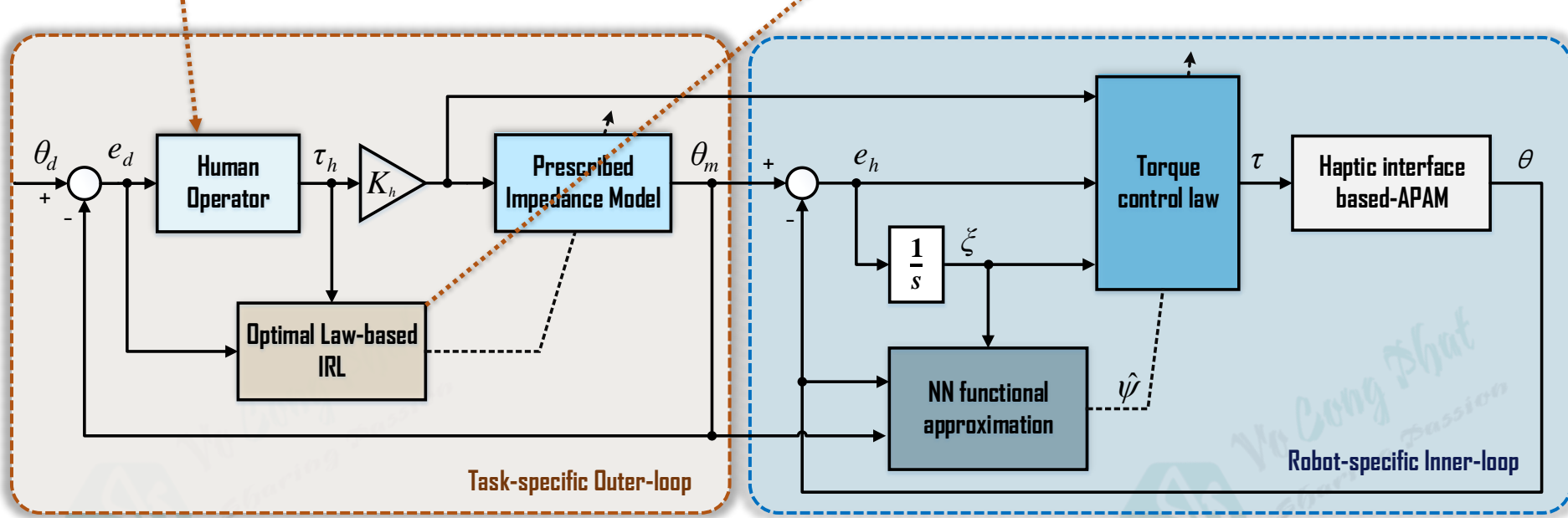
$$\dot{\tau}_h = A_h \tau_h + B_h \bar{e}_d$$

$$\begin{cases} A_h = -k_e^{-1}, \\ B_h = k_e^{-1} [\kappa_p \quad \kappa_d] \\ \bar{e}_d = [e_d^T \quad \dot{e}_d^T]^T \end{cases}$$

A new augmented state

$$\begin{bmatrix} \dot{\bar{e}}_d \\ \dot{\tau}_h \end{bmatrix} = \begin{bmatrix} A_q & 0 \\ B_h & A_h \end{bmatrix} \begin{bmatrix} \bar{e}_d \\ \tau_h \end{bmatrix} + \begin{bmatrix} B_q \\ 0 \end{bmatrix} u_e \Leftrightarrow \begin{cases} \dot{X} = AX + Bu_e \\ u_e = -KX \end{cases}$$

IRL based on LQR solution



6. OPTIMIZED HUMAN-ROBOT INTERACTION FORCE CONTROL USING IRL

Control design

RL solution

A new augmented state

$$\begin{cases} \dot{\bar{X}} = \begin{bmatrix} \dot{\bar{e}}_d \\ \dot{\tau}_h \end{bmatrix} = \begin{bmatrix} A_q & 0 \\ B_h & A_h \end{bmatrix} \begin{bmatrix} \bar{e}_d \\ \tau_h \end{bmatrix} + \begin{bmatrix} B_q \\ 0 \end{bmatrix} u_e \\ u_e = -KX \end{cases}$$

To minimize

The performance index

$$J_m = \int_t^{\infty} (\bar{e}_d^T Q_d \bar{e}_d + \tau_h^T Q_h \tau_h + u_e^T R u_e) d\chi$$

The algebraic Riccati equation [83]

$$0 = A^T P + PA + Q - PB^T R^{-1} BP$$

An optimal feedback control

$$u_e^* = \arg \min_{u_e(\chi), t \leq \chi \leq \infty} V(t, X(t), u_e(\chi)) = -R^{-1} B^T P X$$



IRL solution

The infinite-horizon quadratic cost

$$V_7(X(t)) = \int_t^{\infty} X^T(\chi) (Q + K^T R K) X^T(\chi) d\chi = X^T P X$$

where P is the real symmetric positive definite solution

$$(A - BK)^T P + P(A - BK) = -(Q + K^T R K)$$

The IRL Bellman equation for time interval $\Delta T > 0$

$$V_7(X(t)) = \int_t^{t+\Delta T} X^T(\chi) (Q + K^T R K) X^T(\chi) d\chi - V_7(X(t + \Delta T))$$

The IRL Bellman equation can be written as

$$X(t)^T P X(t) = \int_t^{t+\Delta t} X^T(\chi) (Q + K^T R K) X^T(\chi) d\chi + X^T(t + \Delta t) P X(t + \Delta t)$$

Proof of convergence: See in Appendix 6.2.

6. OPTIMIZED HUMAN-ROBOT INTERACTION FORCE CONTROL USING IRL

Control design

Online implementation

1. Start with an admissible control input

$$u_e^0 = -K_1^0 X$$

2. **Policy evaluation:** given a control policy u^i , find the P^i using off-policy Bellman equation

$$X(t)^T P^i X(t) = \int_t^{t+\Delta t} X^T(\chi) \left(Q + \left(K^i \right)^T R K^i \right) X^T(\chi) d\chi + X^T(t + \Delta t) P^i X(t + \Delta t)$$

3. **Policy Improvement:** update the control policy

$$u_e^{i+1} = -R^{-1} B_1^T P^i X$$

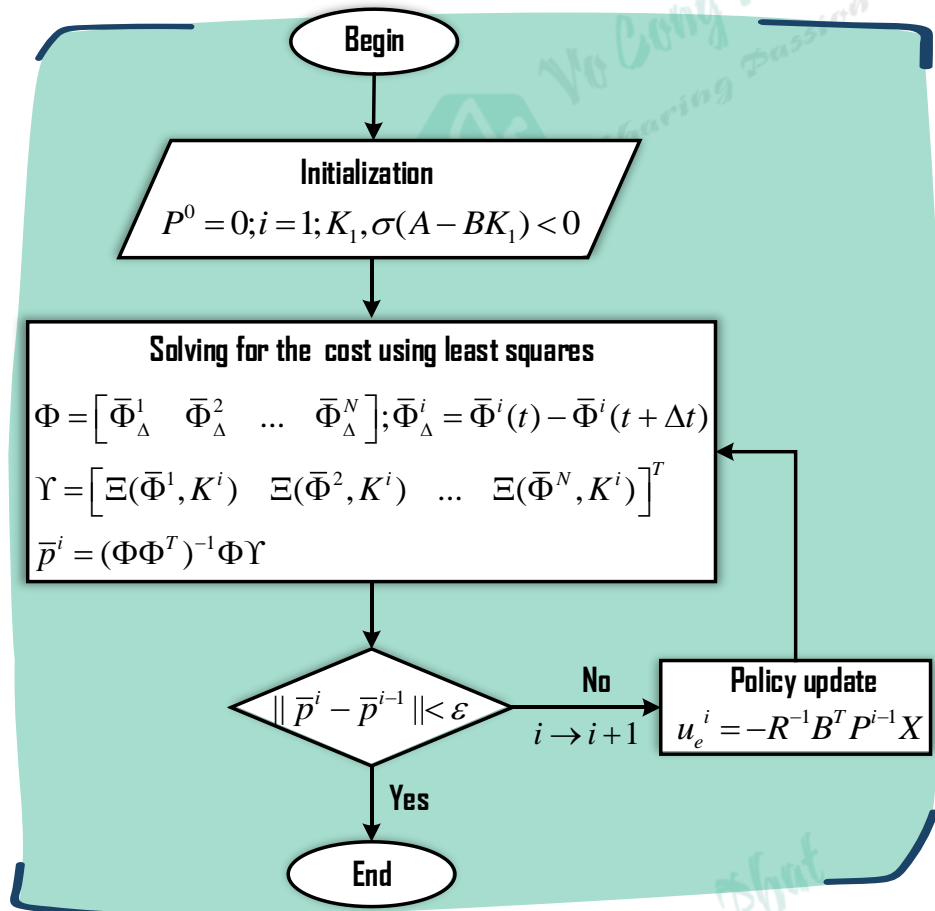


Fig. 6.1. Continuous-time linear policy iteration algorithm.



Validation results

Simulation



Parameters

$$\theta_d = 10\sin(0.2\pi t), M_d = 1 \text{ Kg}, B_d = 7.18 \text{ N.s.mm}^{-1}, K_d = 15.76 \text{ N.mm}^{-1}, K_h = 0.046.$$

Position control:

$$K_s = 20, F = 10, G = 1, \mu_1 = \mu_2 = 5, k = 0.1, \bar{Z} = 100, \kappa_p = 20, \kappa_d = 10 \text{ and } k_e = 0.18 \text{ s}$$

LQR solution:

$$\kappa_e = 0.0025, S = 1, R = 10, T = 0.001, A = -4.006, B = -0.002$$

RL approximation:

$$v = 0.9, \gamma = 0.9, \delta_\Delta = 0.65, \varepsilon = 0.1, \varepsilon\text{-decay} = 0.99, K = 10, \beta = 0.1$$

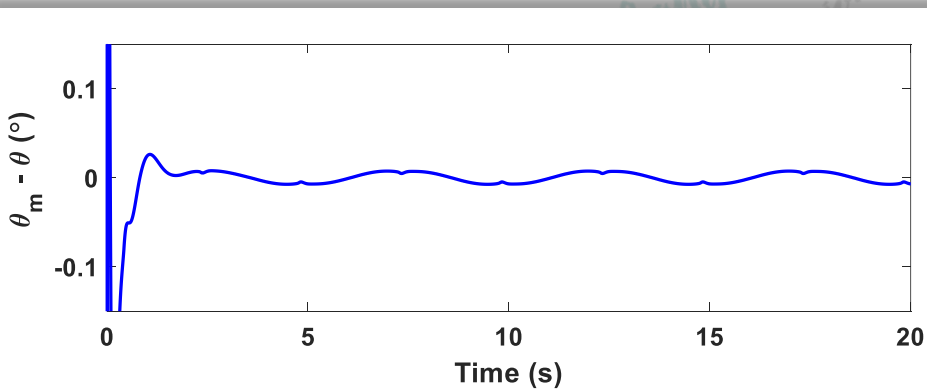


Fig. 6.2. The tracking error of the trajectory of the robot system and the prescribed impedance model.

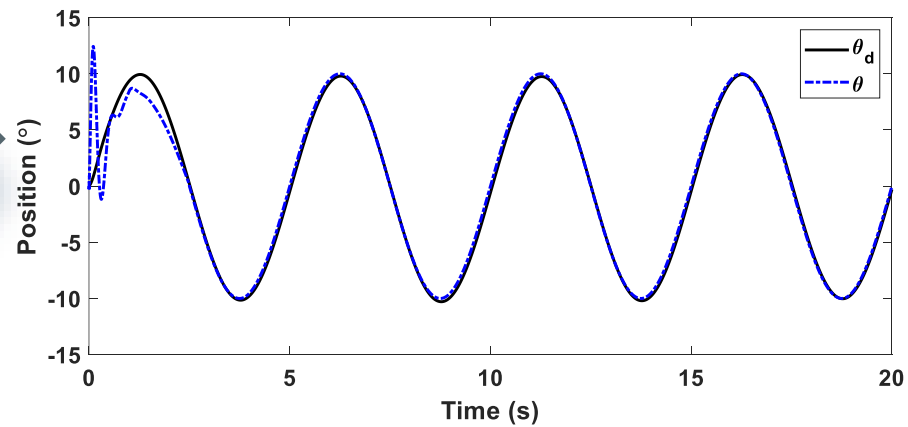


Fig. 6.3. Reference trajectory versus the state of the robot systems during and after learning.

6. OPTIMIZED HUMAN-ROBOT INTERACTION FORCE CONTROL USING IRL



Validation results

Experiment



Discussion

Perfectly performance of the human-robot cooperation.

A little deviation between the desired and actual trajectory.

The human interaction force is reduced after learning and the optimal set of the prescribed impedance model is found by the outer-loop controller

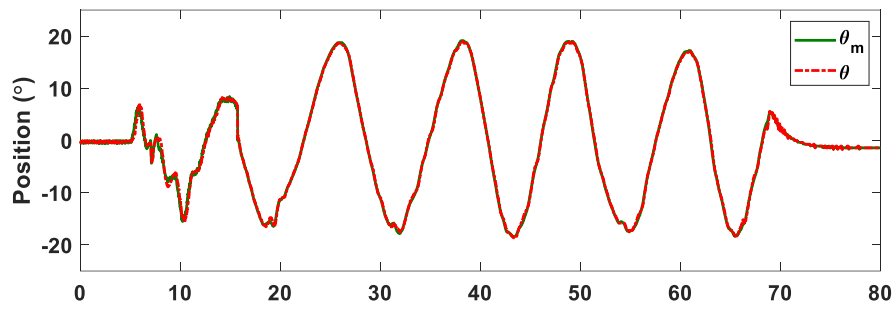


Fig. 6.4. The output trajectory and impedance model in the inner loop

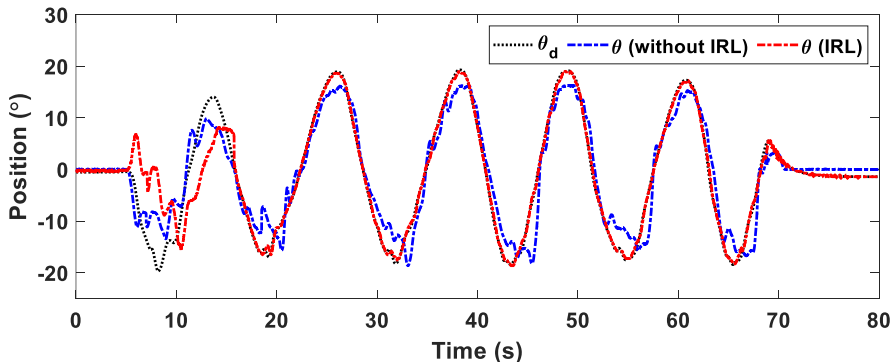


Fig. 6.5. The desired trajectory and output trajectory the outer loop

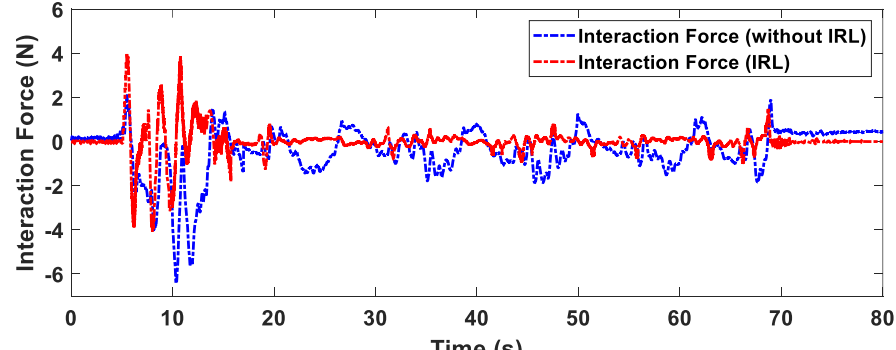


Fig. 6.6. Interaction force.

C H A P T E R

1

Introduction

2

Modeling and platform setup based on the APAM configuration

3

Adaptive Gain ITSMC with TDE scheme

4

Adaptive Finite-Time Force Sensorless Control scheme

5

Model-free control for Optimal contact force in Unknown Environment

6

Optimized Human-Robot Interaction force control using IRL

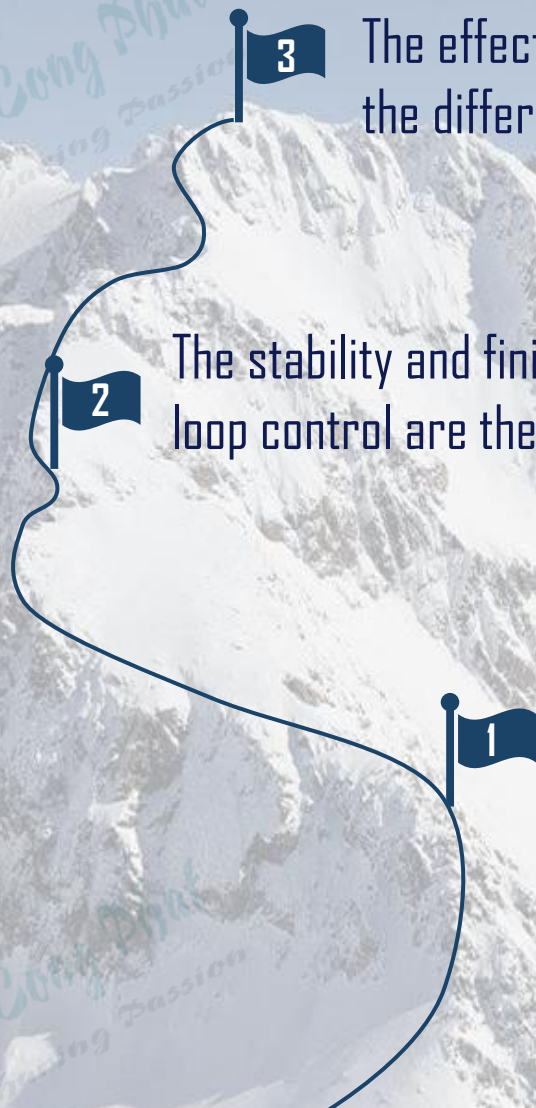
7

Force Sensorless Reflecting Control for BHTS

8

Conclusion and Future works

Proposed control idea



1 The first time the hybrid control based on a fast finite-time NTSMC and AFDOB

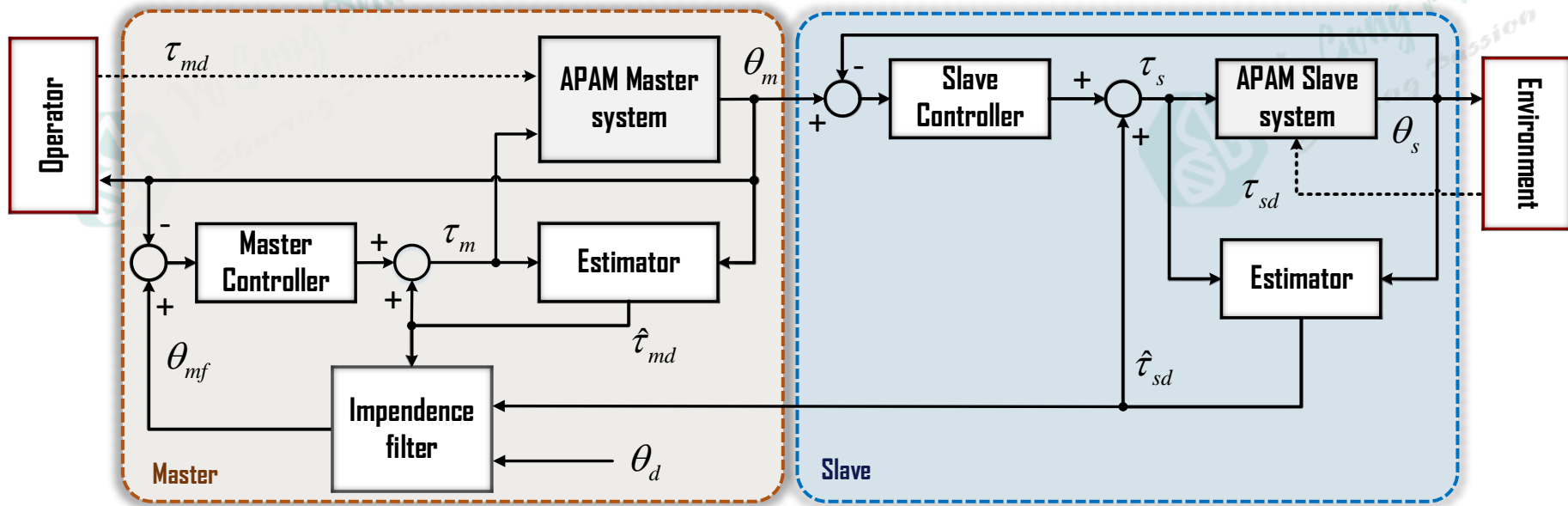
2 The stability and finite-time convergence characteristic of the closed-loop control are theoretically analyzed by the Lyapunov approach

3 The effectiveness of the proposed control method is verified in the different working conditions



7. FORCE SENSORLESS REFLECTING CONTROL FOR BHTS

Control design



The external torque estimation

$$\dot{\tilde{\tau}}_{id} = -\delta\kappa(\Gamma_1 + \eta\Gamma_2)$$

where $\begin{cases} \Gamma_1 = -\Upsilon_1 \tilde{\tau}_{id} + \Omega \\ \Gamma_2 = -\sigma_i^{*T} \sigma_i^* \tilde{\tau}_{id} + \sigma_i^* \psi \end{cases}$

An adaptive FSQB gain

$$\dot{\kappa} = a\kappa - \kappa\sigma_i^{*T} \sigma_i \kappa$$

The torque control design by style-FNTSMC

$$\tau_i = \bar{M}_i \ddot{\tilde{\theta}}_{ir} + \bar{C}_i \dot{\tilde{\theta}}_i + \bar{K}_i \tilde{\theta}_i - \varepsilon_i \text{sign}(s_i) - \rho_{1i} s_i - \rho_{2i} s_i^{[v_i]} + \hat{\tau}_{id}$$

The modified FNTSM surface design

$$s_i = \Pi_i(\tilde{\theta}_i) + \dot{\tilde{\theta}}_i$$

where $\Pi_i(\tilde{\theta}_i) = \begin{cases} \lambda_i \tilde{\theta}_i^{[\alpha_i]}, & \text{if } s_i = 0 \text{ or } s_i \neq 0 \text{ and } |\tilde{\theta}_i| > \varsigma_i \\ z_{1i} \tilde{\theta}_i + z_{2i} \tilde{\theta}_i^2 \text{sign}(\tilde{\theta}_i), & \text{if } s_i \neq 0 \text{ and } |\tilde{\theta}_i| \leq \varsigma_i \end{cases}$

Validation results



Parameters

Observers:

for NDO: $L_h = L_e = 10$; for RTOB: $\beta = 350 \text{ rad/s}$;
 for AFDB: $\kappa_i(0) = 0.1$, $\lambda_i = 10$, $\eta_i = 0$, $m = 0.1$,
 $a = 10$.

PID control:

$K_P = 3.8$, $K_I = 25$, $K_D = 0.15$;

Proposed control:

$\lambda_i = 8$, $p_i = 5$, $q_i = 7$, $\varsigma_i = 10^{-4}$, $v_i = 9/11$,
 $\varepsilon_i = 0.1$, $\rho_{1i} = 10$, $\rho_{2i} = 2$.

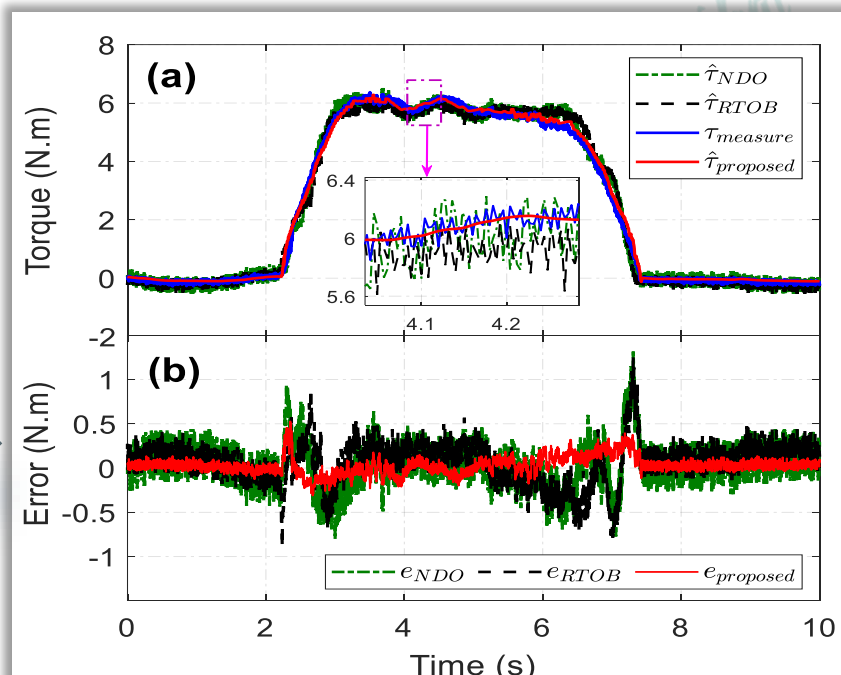


Fig. 7.1. Torque estimation performances.

Scenarios:

- The free space situation $\theta_d(t) = 5\pi \cdot (1 - 0.18t) \cdot \sin(0.72\pi t)$.
- The contact and recovery situation: soft environment $K_e = 500 \text{ N.mm}^{-1}$, $B_e = 4 \text{ N.s.mm}^{-1}$
 stiff environment $K_e = 2800 \text{ N.mm}^{-1}$, $B_e = 20 \text{ N.s.mm}^{-1}$

RMSEs associated with NDO, RTDB and proposed algorithm are calculated of 0.211, 0.192 and 0.076, respectively.

7. FORCE SENSORLESS REFLECTING CONTROL FOR BHTS



Validation results

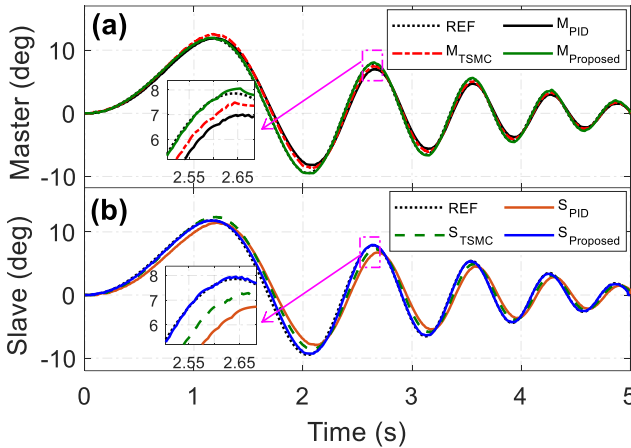


Fig. 7.2. Position tracking performances.

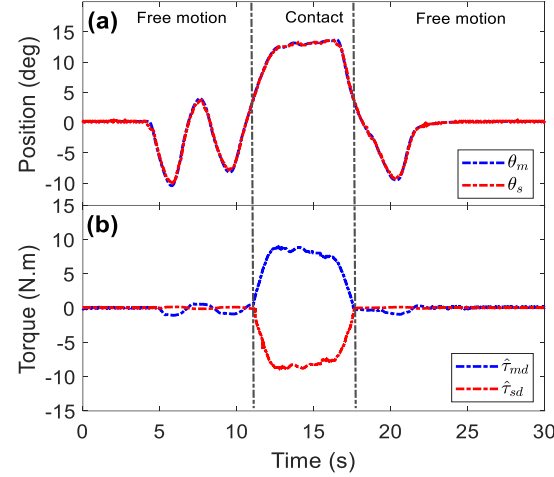


Fig. 7.2. Transparency performance in "soft"

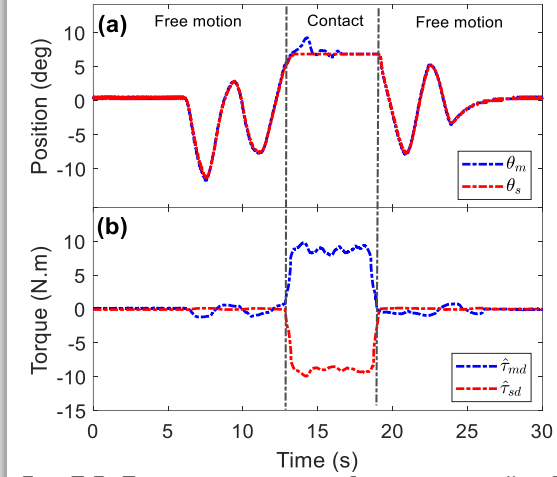


Fig. 7.2. Transparency performance in "stiff"

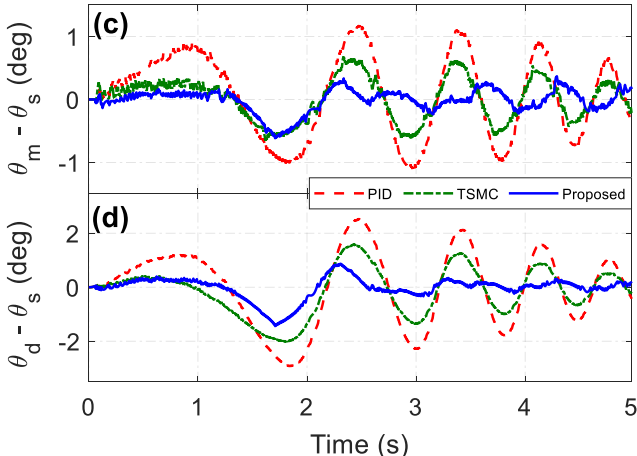


Fig. 7.2. Position tracking error performances.

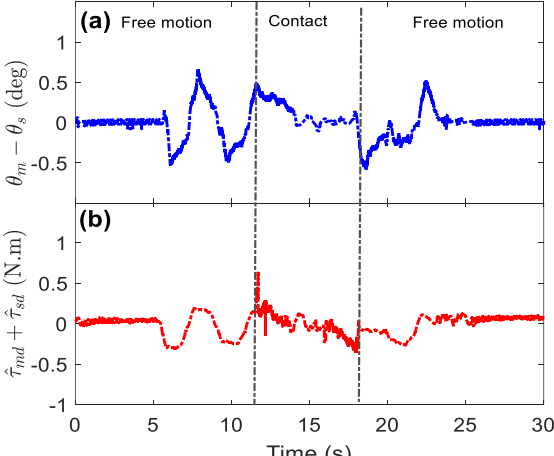


Fig. 7.2. Transparency error in soft contract

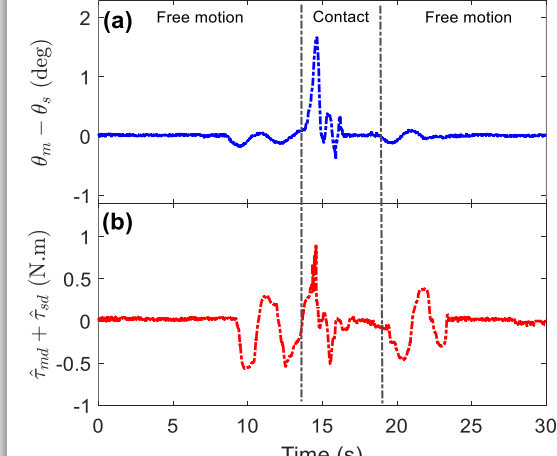


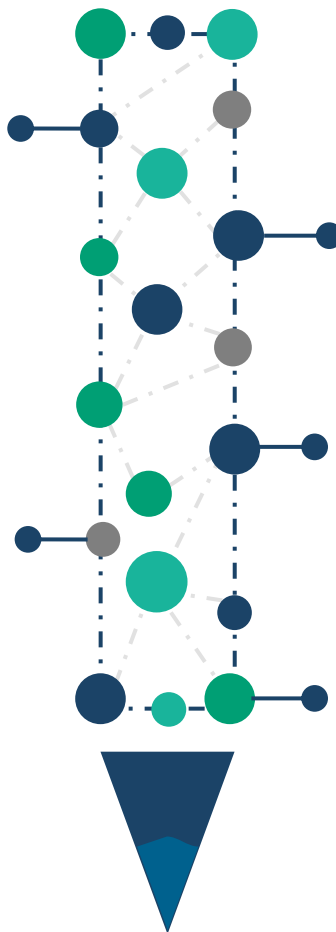
Fig. 7.2. Transparency error in stiff contract

7. FORCE SENSORLESS REFLECTING CONTROL FOR BHTS

Summary

Robust performance against uncertainties and disturbances in the system dynamics

Stability of the overall system and the transparency performance can be attained simultaneously

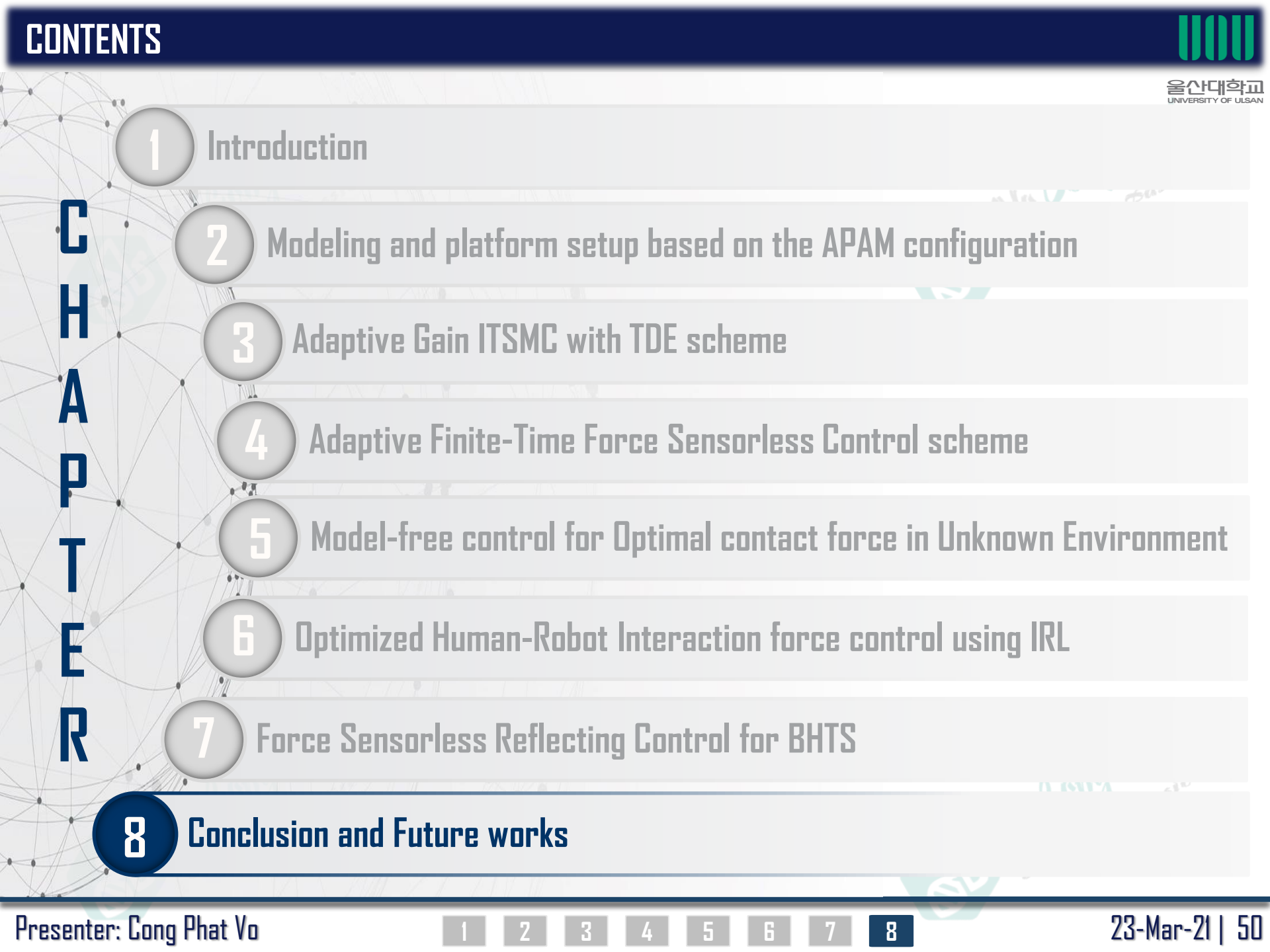


Eliminating the uncertainties the noise effect in the obtained force sensing via new AFOB

Finite-time convergence of the tracking errors

Fast transient response

The great transparency performance and global stability of the BHTS under the proposed control scheme are achieved despite the uncertainties and in different working conditions.

- 
- C H A P T E R**
- 1 Introduction**
 - 2 Modeling and platform setup based on the APAM configuration**
 - 3 Adaptive Gain ITSMC with TDE scheme**
 - 4 Adaptive Finite-Time Force Sensorless Control scheme**
 - 5 Model-free control for Optimal contact force in Unknown Environment**
 - 6 Optimized Human-Robot Interaction force control using IRL**
 - 7 Force Sensorless Reflecting Control for BHTS**
 - 8 Conclusion and Future works**



Conclusions



Verified an effective position tracking controller via the AITSMC with TDE technique under various working conditions (Its uncertainties and disturbance are handled)



Validated the significant effectiveness of finite-time force tracking problems based on the FITSMC combined with a new adaptive gain and a friction-free disturbance (FSOB)



Based on the online learning ability of the RL approximation method, the model-free controller for optimal contact force ensures great position and force tracking performance



Optimized a prescribed impedance model parameters by the IRL approach to provide little operator information in yielding highly effective position control purpose



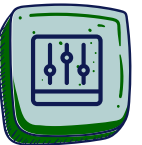
Achieved good transparency performance with both force feedback and position tracking simultaneously by the new adaptive force estimation combined the separately FNTSMC schemes



Future works



To improve the control performance in joint-space, the robot system model can be improved by robust identification approaches.



Effectiveness of the proposed algorithm can be further increased by developing an automatic tune method for both the estimation and control gains.



Apply optimized strategies on both master and slave sides. Note also that the computational complexity should be reduced by the data size



Based on the developed prototype in this thesis, it is possible to develop a high-quality commercial teleoperation device in the rehabilitation field with a safer solution.

❖ International Journals

1. C. P. Vo, M. Shahriar, C. D. Le, and K. K. Ahn, "Mechanically Active Transducing Element Based on Solid–Liquid Triboelectric Nanogenerator for Self-Powered Sensing", *Int. J. Pr. Eng. Man.-GT*, 2019. (IF: 4.561)
2. M. Shahriar, C. P. Vo, and K. K. Ahn, "Self-powered Flexible PDMS Channel Assisted Discrete Liquid Column Motion Based Triboelectric Nanogenerator as Mechanical Transducer", *Int. J. Pr. Eng. Man.-GT*, 2019. (IF: 4.561)
3. C. P. Vo, X. D. To, and K. K. Ahn, "A Novel Adaptive Gain Integral Terminal Sliding Mode Control scheme of a Pneumatic Artificial Muscle system with Time-delay Estimation", *IEEE Access*, 2019. (IF: 4.098)
4. C. P. Vo, X. D. To, and K. K. Ahn, "A Novel Force Sensorless Reflecting Control for Bilateral Haptic Teleoperation System", *IEEE Access*, 2020. (IF: 4.098)
5. G. H. Nam, J. H. Ahn, G. H. Lee, C. P. Vo, and K. K. Ahn, "A New Pathway for Liquid-Solid Triboelectric Nanogenerator Using Streaming Flow by a Novel Direct Charge Transfer", *Adv. Energy Sustainability Res.*, 2020.
6. C. D. Le*, C. P. Vo*, T. H. Nguyen, D. L. Vu, and K. K. Ahn, "Liquid-Solid Contact Electrification Based on Discontinuous-Conduction Triboelectric Nanogenerator Induced by Radially Symmetrical Structure", *Nano Energy*, 2020. (IF: 16.602)

❖ International Conferences

1. C. P. Vo, D. T. Tran and K. K. Ahn, "The Predictive Control for Networked Control System with Random Delays and Packet Dropouts," in 2018 22nd International Conference on Mechatronics Technology (ICMT), Jeju, South Korea, Oct. 2018.
2. C. P. Vo and K. K. Ahn, "High-precision Position Control of Soft Actuator Systems, " The 3rd International Workshop on Active Materials and Soft Mechatronics (AMSM2018), KAIST, Daejeon, South Korea, Oct. 2018.
3. D. T. Tran, C. D. Le, C. P. Vo and K. K. Ahn, "Robust network predictive control of DC motor with delay and drop out," in 2018 22nd International Conference on Mechatronics Technology (ICMT), Jeju, South Korea, Oct. 2018.
4. C. P. Vo, X. D. To, and K. K. Ahn, "Variable Impedance Control for a Robotic Leg with External Uncertainties," in 2019 23rd International Conference on Mechatronics Technology (ICMT), SALERNO, Italy, Oct. 2019.

A PRESENTATION OF DOCTORAL DISSERTATION

Department of Mechanical Engineering, University of Ulsan, Korea

Thank you for attending!